

A comprehensive review on fish-inspired robots

Yi Li^{1,2} , Yuteng Xu^{1,2}, Zhenguo Wu^{1,2}, Lei Ma^{1,2}, Mingfei Guo^{1,2},
Zhixin Li^{1,2} and Yanbiao Li^{1,2}

International Journal of Advanced
Robotic Systems

May-June 2022: 1–20

© The Author(s) 2022

Article reuse guidelines:

sagepub.com/journals-permissions

DOI: 10.1177/17298806221103707

journals.sagepub.com/home/arx



Abstract

Recently, the increasing interest in underwater exploration motivates the development of aquatic unmanned vehicles. To execute hazardous tasks in an unknown or even hostile environment, researchers have directed on developing biomimetic robots inspired by the extraordinary maneuverability, cruising speed, and propulsion efficiency of fish. Nevertheless, the performance of current prototypes still has gaps compared with that of real fishes. In this review, recent approaches in structure designs, actuators, and sensors are presented. In addition, the theoretical methods for modeling the robotic fishes are consolidated, and the control strategies are offered. Finally, the current challenges are summarized, and possible future directions are deeply discussed. It is expected that the emergence of new engineering and biological technologies will enhance the field of robotic fish for further advancement.

Keywords

Underwater robot, bionic robotic fish, locomotion, actuators, modeling, control

Date received: 20 December 2021; accepted: 09 May 2022

Topic: Bioinspired Robotics

Topic Editor: Chin-Hsing Kuo

Associate Editor: Hoon Cheol Park

Introduction

Under the thousands of years of natural selection, the fishes in nature have been endowed with great locomotion capabilities, such as high swimming speed and remarkable maneuverability, prompting researchers to develop various types of fish-inspired underwater robots.¹ Compared with conventional underwater vehicles powered by screw propellers, robotic fish can overcome their shortcomings, such as large scale, low energy efficiency, and disturbance to the environment, and it has great superiority in propulsive efficiency, maneuverability, and stealth.^{2,3} With the development of mechatronic technologies and computer science, robotic fish plays a huge role in underwater exploration,^{4–6} samplings,^{7,8} rescues,⁹ and water quality monitoring.¹⁰

The earliest research on fish can be traced back to 1926; Breder¹¹ categorized the swimming modes of fishes into the body and/or caudal fin (BCF) propulsion and median and/or paired fin (MPF) propulsion according to the body

¹Key Laboratory of Special Purpose Equipment and Advanced Processing Technology of Ministry of Education, Zhejiang University of Technology, Hangzhou, China

²Zhejiang Provincial Key Laboratory of Special Purpose Equipment and Advanced Processing Technology, Zhejiang University of Technology, Hangzhou, China

Corresponding author:

Yi Li, Key Laboratory of Special Purpose Equipment and Advanced Processing Technology of Ministry of Education, Zhejiang University of Technology, Hangzhou 310023, China; Zhejiang Provincial Key Laboratory of Special Purpose Equipment and Advanced Processing Technology, Zhejiang University of Technology, Hangzhou 310023, China. Email: ly17@zjut.edu.cn

Yanbiao Li, Key Laboratory of Special Purpose Equipment and Advanced Processing Technology of Ministry of Education, Zhejiang University of Technology, Hangzhou 310023, China; Zhejiang Provincial Key Laboratory of Special Purpose Equipment and Advanced Processing Technology, Zhejiang University of Technology, Hangzhou 310023, China. Email: lybrory@zjut.edu.cn



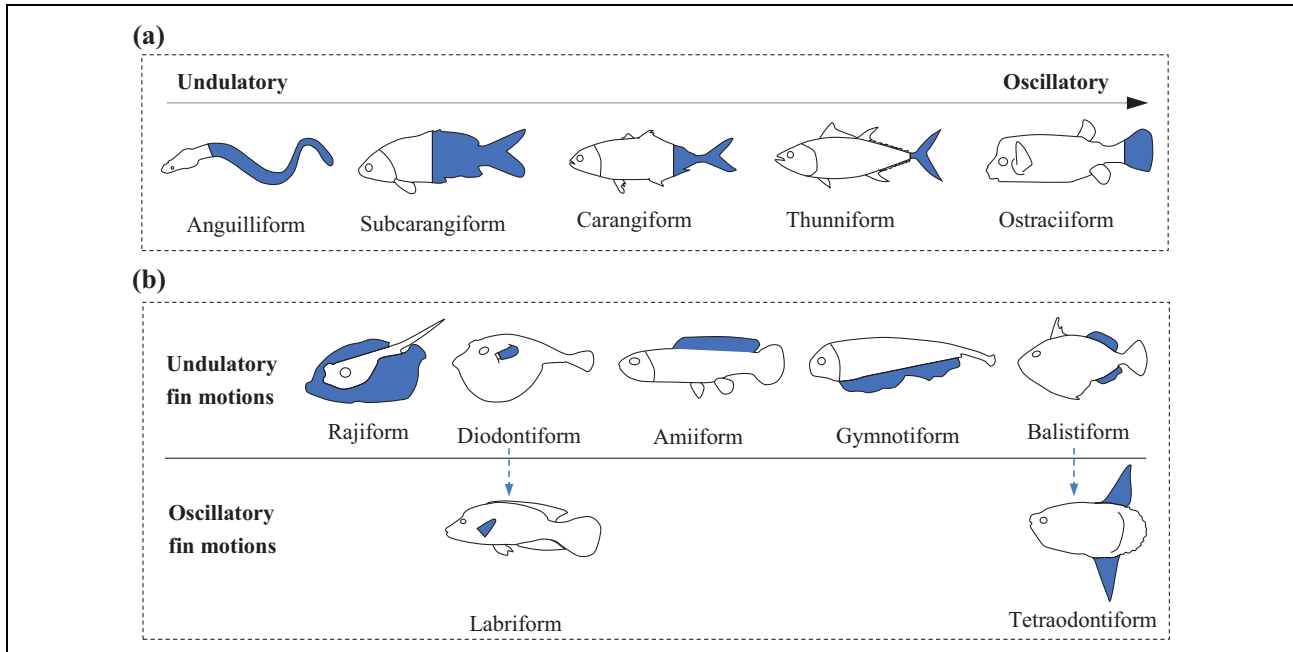


Figure 1. Classification of swimming modes: (a) BCF and (b) MPF. Blue areas contribute to swim. Adapted and redrawn from Ref.³² BCF: body and/or caudal fin; MPF: median and/or paired fin.

part utilized for propulsion. In 1936, through the observation of dolphins, Gary¹² calculated that dolphins need only one-seventh of the external force generated by their muscles to maintain a high swimming speed. This finding motivated researchers to study the mechanism of fish swimming. In the 1960s, some progress had been made in the theoretical study of fish propulsion. The theories could be categorized into resistive force theory¹³ and reactive force theory.^{14–18} The former emphasizes the viscous force, while the latter emphasizes the more accurate inertia force. There are three kinds of reactive force theories that are relatively widely used in fish dynamic modeling: elongated body theory (EBT),^{14,18} wave plate theory (WPT),^{15,16} and actuator-disc theory.¹⁷ In 1995, based on previous studies, the first complete robotic fish system named RoboTuna¹⁹ was developed by Massachusetts Institute of Technology (MIT). Since then, many related studies have been carried out, and the latest research results have been applied to the design of robotic fish.²⁰ Various types of fish-like robots have sprung up endlessly.^{21–24}

To meet the increasing requirements of underwater missions, new approaches have been constantly proposed in design aspects. Recent advances in smart materials and actuators and compliant mechanisms have boosted the research studies on the mechanical design of robotic fishes.²⁵ Many smart control strategies are applied to improve the robotic performance, and closed-loop control based on onboard sensors is used to realize the precise control.²⁶ These approaches have been reviewed in recent articles,^{26–31} but few of them give an overall description.

Salazar et al.²⁷ reviewed the modeling, materials, and actuators, but there is no mention of sensors and control. Xie et al.³¹ reviewed the robotic fishes with different mechanisms in detail, but the control strategy is not deeply discussed. Yu et al.²⁶ offered a detailed review of control strategies, but the other aspects are not declared. Differently, this article focuses on the recent studies and gives a relatively overall review. The motivation is to provide a relevant and useful introduction to the state-of-the-art robotic fish and to inspire researchers to explore the opportunities for further improvement and novel designs in robotic fish from existing studies.

The remainder of this article is organized as follows: The movement characteristics of different types of fishes are summarized, and recent typical designs are given in the second section. Smart soft actuators with properties and limitations for propulsion are detailed in the third section. The applications of sensors in robotic fish are provided in the fourth section. Typical modeling and control methods are proposed, and related theoretical research studies are sorted out in the fifth section. In addition, possible future challenges and directions are discussed in the sixth section. Finally, conclusions are given in the seventh section.

Robotic fish designs based on different locomotion modes

As stated in the previous section, the swimming modes of fish can be categorized into BCF propulsion and MPF propulsion. The BCF mode is suitable for long-term swimming

Table 1. Performance and characteristics of the BCF mode-based robotic fishes.

Fish type	Prototypes	Speed (BL/s)	Characteristics
Anguilliform	Envirobot ³³	1.0	<ul style="list-style-type: none"> • Six active modules, a passive flexible tail • Each module is powered by a dc motor • The core component is a helix actuated by a single dc motor
	MAR ³⁴	0.44	
Subcarangiform or carangiform	Isplash-II ³⁵	11.6	<ul style="list-style-type: none"> • 15 rectangular elements to hold the helix • A single motor and three passive links • Cruise straight only • Wire-driven active body and compliant tail
	Compliant robot ³⁶	2.15	
Thunniform	SPC-III ⁵	0.77	<ul style="list-style-type: none"> • The multi-pseudo-link model • A parallel four-bar linkage mechanism • Actuated by two dc servomotors
	Robot by Algarin-Pinto ³⁷	Not available	
Ostraciiform	Robot by Costa ³⁸	0.42	<ul style="list-style-type: none"> • A 3ucul s parallel mechanism • Oscillatory motion only • A cylindrical rigid fore body and a tail section • A cam-like mechanism powered by a DC brushed motor
	Robot by Zhang ³⁹	2.0	

BCF: body and/or caudal fin; MAR: marine anguilliform robot.

Table 2. Performance and characteristics of the MPF mode-based robotic fishes.

Fish type	Prototypes	Speed (BL/s)	Characteristics
Rajiform	Roman-II ⁴⁰	0.8	<ul style="list-style-type: none"> • Three parallel and compliant fin rays • Slider-rocker mechanisms of fin rays • Tiny and soft • Four layers assembled • Steering upon optical stimulation
	Cownose ray inspired robot ⁴¹	0.7	
	Tissue-engineered robotic ray ⁴²	0.20	
Amiiform	Robognilos ⁴³	0.87	<ul style="list-style-type: none"> • Nine fin rays directly attached to the servo motors • An asymmetrical sinusoidal profile of propulsion waveform • 32 fin rays actuated by 32 motors • A cylindrical and rigid body • 16 fin rays actuated by 32 motor units • Oval-shaped cross-section rigid body • The fin membrane is passively undulated by crank–slider mechanisms • A caudal fin to aid with forward thrust
Gymnotiform	Robotic knifefish ⁴⁴	0.55	
	Knifebot ⁴⁵	0.37 (forward) 0.25 (backward) 0.20 (vertical)	
	Fin-rayless robot ⁴⁶	0.21	
Labriform	Flexible feathering fin robot ⁴⁷	0.17	<ul style="list-style-type: none"> • Rigid rectangular fins • Flexible feathering joints • Trapezoidal folding fins • Flexible joints on hinge base
	Flexible folding fin robot ⁴⁸	0.58	

MPF: median and/or paired fin.

using the caudal fin to produce large thrust, whereas the MPF mode uses paired pectoral fins, dorsal fins, or anal fins to obtain sufficient maneuverability. As shown in Figure 1,³² based on the difference between undulatory and oscillatory motion, BCF mode could be further classified into anguilliform, subcarangiform, carangiform, thunniform, and ostraciiform. MPF mode could be further classified into rajiform, diodontiform, labriform, amiiform, gymnotiform, balistiform, and tetraodontiform. Typical prototypes based on each category (as presented in Tables 1 and 2) are deeply discussed in this section.

BCF mode-based robotic fishes

Swimming in anguilliform mode is based on axial waves propagating along the body from head to tail, and the wave number is about one body length.⁴⁹ Hyper-redundant design is usually used in robots inspired by anguilliform to obtain high maneuverability. Envirobot developed by Bayat et al.³³ is composed of six active modules, a passive flexible tail, and an un-actuated head module (see Figure 2(b)). Struebig et al.³⁴ developed a new anguilliform swimming robot—named Marine Anguilliform Robot

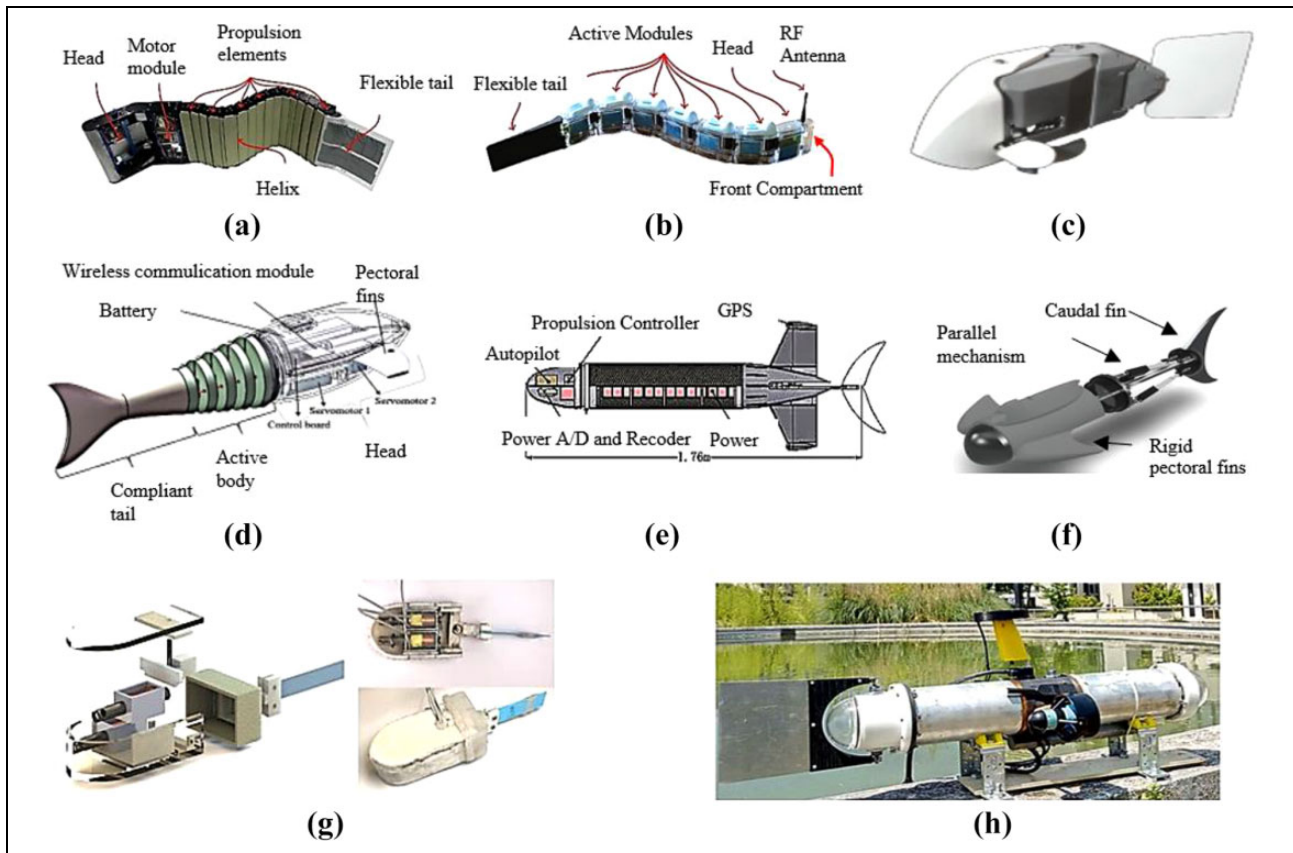


Figure 2. Robotic fish prototypes based on different BCF modes: (a) MAR. Reproduced with permission.³⁴ Copyright 2019, IOP Publishing. (b) Envirobot. Reproduced with permission.³³ Copyright 2021, IEEE. (c) iSplash-II. Reproduced with permission.³⁵ Copyright 2014, IEEE. (d) Compliant robot. Reproduced with permission.³⁶ Copyright 2017, IEEE. (e) SPC-III. Reproduced with permission.⁵ Copyright 2011, Wiley. (f) Robot by Algarin-Pinto. Reproduced with permission.³⁷ Copyright 2021, MDPI. (g) Robot by Zhang. Reproduced with permission.³⁹ Copyright 2018, IEEE. (h) Robot by Costa. Reproduced with permission.³⁸ Copyright 2014, Springer. BCF: body and/or caudal fin; MAR: marine anguilliform robot.

(MAR) (see Figure 2(a)). Different from hyper-redundant mechanisms, the core component of the robot is a helix. Several rectangular elements are adopted to project the three-dimensional rotation of the helix onto the vertical plane, and thus, a continuous traveling wave can be created. Since the robot is actuated by a single DC motor installed on the head, the efficiency of the robot is improved, and the control strategy is significantly simplified. However, the overall scale is relatively large (108 cm, 5.5 cm, and 25 cm in length, width, and height, respectively), and waterproof measures of each element are lacking, which leads to a large friction force in swimming.

In contrast to anguilliform that the whole body participating in undulation, the undulations in subcarangiform and carangiform are confined to the posterior half and the latter third of body length, respectively, while the nonundulating parts of both remain almost rigid.⁵⁰ As a result, the swimming speed is higher than that of the anguilliform while the maneuverability is lower.⁵¹ Multi-joint mechanism is usually utilized to fit the movement of the counterpart fish.^{52–54} The iSplash-II developed by Clapham et al.³⁵ is well known for its high speed (up to 11.6 body length (BL)

per second at the frequency of 20 Hz) (see Figure 2(c)). However, it can only realize linear locomotion but can not maneuver in 3D space. Zhong et al.³⁶ developed a novel robotic fish (see Figure 2(d)) with wire-driven active body and compliant tail, which were driven, respectively, by two servo motors housed in the head. The active body consists of five joints, and it could be bent in a C-shape and the soft compliant tail lags behind, resulting in an S-shape of the robot.

The fish swimming in thunniform mode has a crescent-shaped caudal fin with a high aspect ratio connected to a narrow peduncle.¹² Significant transverse movement occurs in the peduncle, and the tail area when swimming while the anterior body remains rigid,⁵⁵ which leads to high speed with high efficiency. Since only the rear 10% of the body participates in oscillation, the torpedo-shaped SPC-III developed by Liang et al.⁵ uses a parallel four-bar linkage mechanism actuated by two DC servomotors to oscillate the caudal fin (see Figure 2(e)). Under the lookup-table method control and predictive control, the swimming speed can reach 1.36 m/s with a turning radius of 1.75 m, and the robotic fish can be operated for up to 20 h powered by the

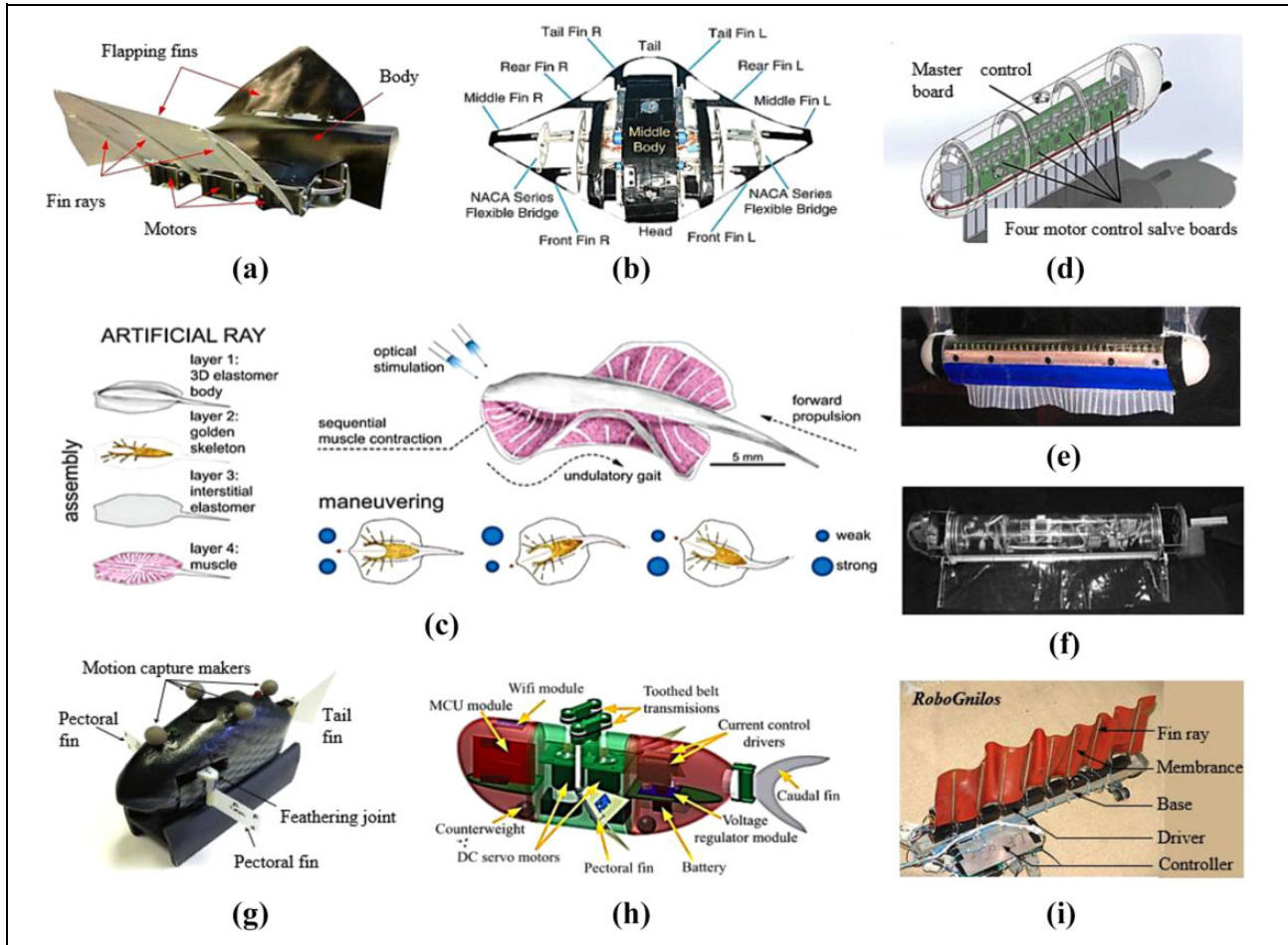


Figure 3. Robotic fish prototypes based on different MPF modes: (a) Roman-II. Reproduced with permission.⁴⁰ Copyright 2012, IEEE. (b) Cownose ray inspired robot. Reproduced with permission.⁴¹ Copyright 2019, IEEE. (c) Tissue-engineered robotic ray. Reproduced with permission.⁴² Copyright 2016, Amer Assoc Advancement Science. (d) Knifebot. Reproduced with permission.⁴⁵ Copyright 2018, IOP publishing. (e) Robotic knifefish. Reproduced with permission.⁴⁴ Copyright 2011, Royal Soc. (f) Fin-rayless robot. Reproduced with permission.⁴⁶ Copyright 2012, IEEE. (g) Flexible feathering fin robot. Reproduced with permission.⁴⁷ Copyright 2016, IOP publishing. (h) Flexible folding fin robot. Reproduced with permission.⁴⁸ Copyright 2020, Cambridge Univ Press. (i) Robognilos. Reproduced with permission.⁴³ Copyright 2009, Pergamon-Elsevier Science. MPF: median and/or paired fin.

onboard battery. Pinto et al.³⁷ adopted the three degrees of freedom spherical three universal–cylindrical–universal and one spherical joint (3UCU-1 S) parallel mechanism as the actuation system of robotic fish (see Figure 2(f)). The 3UCU-1 S is driven by linear actuators to mimic the flapping thunniform locomotion, which obtains a high and efficient thrust.

The ostraciiform locomotion is considered the most stable mode as the body parts involved in oscillation is the least. Given to large body shape and inefficient fin actuation, the speed of ostraciiform is relatively low but they can maneuver in a narrow space (almost zero radius⁵⁶) through the fin actuation.⁵⁷ Recently, Costa et al.³⁸ have proposed an ostraciiform robot composed of a cylindrical rigid body and a tail section (see Figure 2(h)). The actuation system is based on a cam-like mechanism powered by a DC brushed motor, which converts the continuous rotation of the drive

into a harmonic oscillation. Zhang et al.³⁹ presented a robot with a 2-segment caudal (see Figure 2(g)). The robot has a large and heavy main body to gain stability, and the caudal fin is actuated by an electromagnetic actuator to obtain higher frequency oscillations (over 50 Hz).

MPF mode-based robotic fishes

Rajiform has a pair of wing-shaped pectoral fins attached to the fin rays extended from the body. Swimming forward and turning are, respectively, realized by flapping and modulating phase relations of fin rays, exhibiting relatively high maneuverability and stability.³² To achieve the rajiform locomotion, the actuation mechanism of the RoMan-II⁴⁰ consists of three parallel and compliant fin rays connected to each side of the body, as shown in Figure 3(a). The fin rays are powered by the brushless servo motors

independently. Hence, the fin membrane attached to them could provide flapping motion. Differently, the fin rays of the robot developed by Cai et al.⁴¹ are not compliant but adopt slider-rocker mechanism to flap in sinusoidal curves (see Figure 3(b)). Specifically, the front fin ray uses a one-stage slide-rocker mechanism, the middle fin ray uses a two-stage slider-rocker mechanism, and the last fin ray uses one linkage. Park et al.⁴² developed a soft-robotic ray with a new design (see Figure 3(c)). The body of the robot is assembled by four layers including a three-dimensional elastomer layer, a chemically neutral skeleton layer, a thin interstitial elastomer layer, and a muscle layer of aligned rat cardiomyocytes. The robot is 16.3 mm in length and about 10.18 mg in weight, which is considered to be the smallest rajiform-inspired prototype. Upon optical stimulation, the metal skeleton induces the bending of the muscle layer to produce undulating locomotion. Consequently, the robot exhibits high maneuverability (turn at 1.5 mm/s), relatively high speed (3.2 mm/s, equal to 0.20 BL/s), and long endurance (6 days).

Amiiform and gymnotiform have similarities in kinematics. Amiiform has a long dorsal fin extending to the entire body length, while gymnotiform has an elongated anal fin. They undulate their fins to swim while their bodies remain rigid. They could smoothly change the gait of swimming forward to backward without turning.^{58,59} Furthermore, they could move vertically by sending inward counter-propagating waves, namely, the traveling wave from head to tail meets the traveling wave from tail to head in the middle of the fin.⁴⁴ Thus, they could maneuver in 3D space easily by controlling the unique long fins. Hu et al.⁴³ developed an amiiform-inspired robot. As shown in Figure 3(i), nine fin rays connecting with a membrane are directly attached to nine servo motors, and the motors are mounted in the long base. As for the gymnotiform, Curet et al.⁴⁴ used 32 fin rays actuated by 32 motors to emulate the dorsal fin. The bionic fin is encased in the cylindrical main body (see Figure 3(e)). Liu et al.⁴⁵ used 16 fin rays independently actuated by motor units (see Figure 3(d)). The fin rays are about 7 cm in length, longer than that of Curet et al.'s 3.4 cm. The robot developed by Liu et al.⁴⁶ adopted the actuation mechanism using no fin rays (see Figure 3(f)). The fin membrane is passively undulated by two crank-slider mechanisms located at the head and the tail, respectively. Moreover, a propulsive caudal fin is also equipped to aid with forward thrust.

Labriform oscillates pectoral fins to generate swimming thrust and occasionally uses caudal fin for rapid acceleration. The movement of pectoral fins is a combination of rowing (vertical rotating axis) and flapping (longitudinal rotating axis) motion to perform slow-speed agile swimming.⁶⁰ Rowing motion including power and recovery strokes is utilized for forward swimming while the flapping for descending or ascending.⁶⁰ The fin mechanism put forward by Behbahani et al.⁴⁷ is about rowing motion. It can be seen in Figure 3(g) that the rigid rectangular fins are

mounted on flexible joints driven by servo motors. The main components of the joint are a mechanical stopper and a rectangular flexible piece. During the power stroke, the mechanical stopper prevents the fin from feathering (transverse rotating axis) and maintains the rowing motion prescribed by the servo motors. In addition, in recovery stroke, the flexible piece makes the fin feather passively, thus reducing the hydrodynamic drag force. Pham et al.⁴⁸ proposed a different fin mechanism in the shape of a trapezoid (less interference drag than a rectangle) (see Figure 3(h)). The pectoral fins are mounted to the hinge base (fin ray) in the middle of the trapezoidal fins through flexible joints. Under this arrangement, the power and recovery strokes can be realized in the form of folding pectoral fins.

However, in diodontiform mode (undulatory pectoral fins), balistiform mode (undulatory anal and dorsal fins), and tetraodontiform mode (oscillatory dorsal and anal fins), there are no robotic systems reported to the authors' knowledge.

Smart soft actuators for propulsion

The traditional motor-driven robotic fish systems are composed of multi-joint body and transmission mechanisms, such as gears, bearings, and pistons, which makes the robots heavy and bulky. In addition, the motors could generate noises and disturb marine life, incapable of integrating into the underwater ecology.⁴ Conversely, the emergence of artificial muscle-based actuators provides a new direction for the development of robotic fish. Although their power and accuracy cannot be compared with motors, smart soft actuators have unique advantages in terms of high deformability and adaptability due to their excellent compliance.⁶¹ Moreover, they could be used as a part of the robot to propel without additional mechanisms. Typical smart soft actuators, such as shape memory alloy (SMA), electroactive polymer (EAP), piezoelectric actuators (PZT), and fluid elastomer actuator (FEA), are reported in robotic fish design, which is discussed in this section. The characteristics of the mainly used smart soft actuators in robotic fish are presented in Table 3.

SMA-based robotic fishes

The principle of SMA is the shape memory effect, namely, the low-temperature martensite reverses into the high-temperature parent phase when heated and returns to the pre-deformation shape during subsequent cooling through the release of internal elastic energy.⁶⁷ SMA can be actuated under a small applied voltage (about 2 V) and generates a high output stress (up to 200 MPa).⁶² SMA is suitable for underwater robots because the surrounding water is a benefit to cooling down the SMA, and faster frequency could be obtained.⁶⁸ SMAs in the form of wire, spring, and plate are found in robotic fish design. Li et al.⁶⁹ attached two SMA wires in the form of a trapezoid (to double the

Table 3. The characteristics of the mainly used smart soft actuators in robotic fish.

Actuator type	Properties	Limitations
SMA ⁶²	<ul style="list-style-type: none"> • Low voltage (2 V) • Strain (4~8%) • High stress (200 MPa) 	<ul style="list-style-type: none"> • Limited frequency (1 Hz) • High driving temperature (over 70 degrees)
IPMC ⁶³	<ul style="list-style-type: none"> • Low voltage (1~3 V) • Strain (>40%) • Low power consumption 	<ul style="list-style-type: none"> • Low stress (0.3 MPa)
PPy ⁶⁴	<ul style="list-style-type: none"> • Fast response • Considerably high strain rate 	<ul style="list-style-type: none"> • Nonlinear hysteresis phenomenon leads to poor controllability
DE ⁶⁵	<ul style="list-style-type: none"> • Fast response (200 μs) • Large actuation strokes (>100%) 	<ul style="list-style-type: none"> • High voltage (>1 KV)
PZT ²⁵	<ul style="list-style-type: none"> • High stress (>110 MPa) • Fast frequency (up to 10000 Hz) 	<ul style="list-style-type: none"> • Small actuation displacement (0.2%) • High voltage (100 V)
FEA ⁶⁶	<ul style="list-style-type: none"> • Helpful to body compliance and mimicry 	<ul style="list-style-type: none"> • Difficulty of power supply

SMA: shape memory alloy; IPMC: ionic polymer-metal composite; PPy: polypyrrole; DE: dielectric elastomer; PZT: piezoelectric actuators; FEA: fluid elastomer actuator.

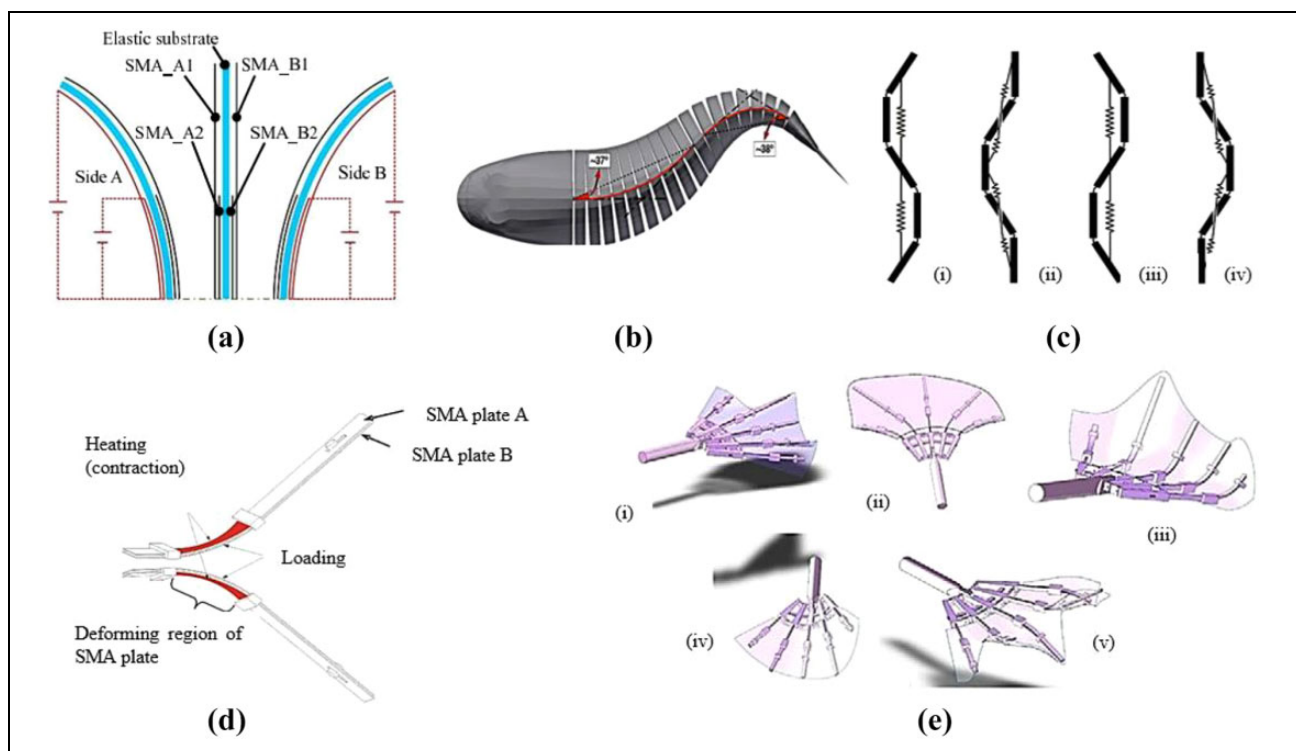


Figure 4. SMA-based robotic fishes: (a) Actuation structure bending to side A and side B, SMA_A1 and SMA_B1 are longer than SMA_A2 and SMA_B2 to undulatory and oscillatory movement.⁶⁹ Copyright 2019, IEEE. (b) A robotic fish based on SMA wires. The dashed line represents the SMA wires, the red line represents the spine, and three types of swimming modes are realized. Reproduced with permission.⁷⁰ Copyright 2018, IOP publishing. (c) The SMAs pass the holes to drive the segments. Reproduced with permission.⁷¹ Copyright 2008, IEEE. (d) Red areas represent deforming regions. Reproduced with permission.⁷² Copyright 2019, Springer. (e) Gestures of a robotic pectoral fin based on observations. (i) relaxation; (ii) expansion; (iii) bending; (iv) cupping; and (v) undulation. Reproduced with permission.⁷³ Copyright 2012, Springer. SMA: shape memory alloy.

stress) of different lengths to each side of an elastic substrate (the backbone of the fishtail) to achieve both undulatory and oscillatory motions (see Figure 4(a)). Coral et al.⁷⁰ adopted 19 ribs and a rigid caudal fin to form the fish body instead of a compliant one. Two groups of SMA wires actuate the fish body and the tail, respectively (see Figure 4(b)).

Notably, the recoverable strain of SMA wires is limited (4–8%). The strain could be substantially improved (up to 200–1000%) when turning the SMA wires to springs, while the generated stress is significantly decreased. Thus, the SMA spring is appropriately adopted in small-size robots. Cho et al.⁷¹ developed a caudal fin propulsion system actuated

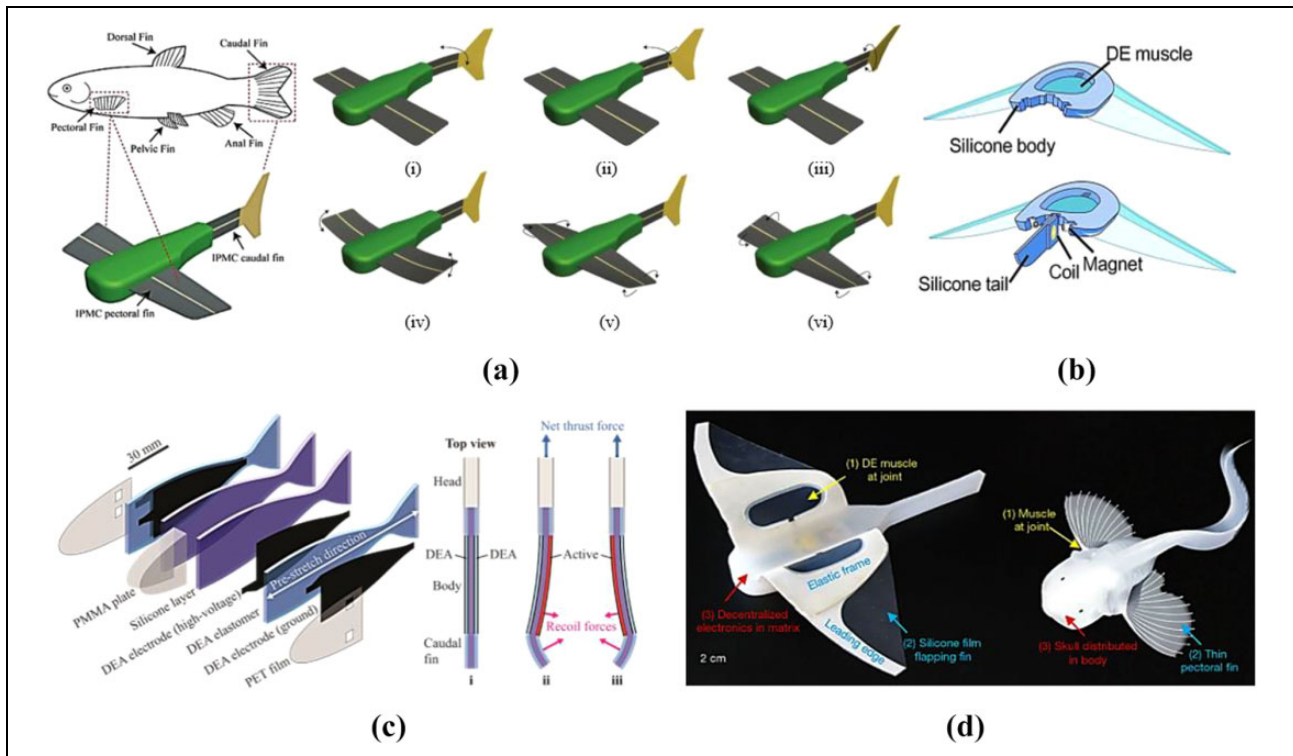


Figure 5. EAPs-based robotic fishes: (a) The deformable IPMCs lead to complex gestures of the robot: (i) Caudal fin bending “flapping”; (ii) caudal fin bending (nonneutral axis) “yaw”; (iii) caudal fin twisting “roll/banking”; (iv) pectoral fin bending “translation/roll/banking”; (v) pectoral fin twisting “pitch-dive/surface”; and (vi) pectoral fin twisting “rolling”. Reproduced with permission.⁸¹ Copyright 2014, IEEE. (b) The structure of the robot: the DE muscle is framed in the silicone body. A silicone tail attached to the body is for steering actuated by a magnet. Reproduced with permission.⁶⁴ Copyright 2017, Amer Assoc Advancement Science. (c) The robot composition: the body is assembled by two DEAs and two silicone layers. The head is made of a PMMA plate and two PET films. The positive DEA electrode is smaller and arranged inside of the body to realize insulation. Actuation structure: (i) pre-stretched state. (ii) and (iii) excited state: flaps the caudal fin to move forward. Reproduced with permission.⁸⁴ Copyright 2021, Mary Ann Liebert. (d) The structure of the self-powered soft robot inspired by snailfish (right). Reproduced with permission.⁶ Copyright 2021, Nature Research. EAP: electroactive polymer; IPMC: ionic polymer metal composite; DEA: dielectric elastomer actuator; PMMA: polymethyl methacrylate; PET: polyethylene terephthalate; DE: dielectric elastomer.

by SMA springs (see Figure 4(c)). The propulsion system is composed of four segments and a caudal fin. The designed spring passes through each joint to drive them to realize subcarangiform movement when heated by wired power.

SMA in the form of a plate is typically adopted to the pectoral fin design. The fin ray developed by Zhang et al.⁷² is composed of two layers of SMA plates sandwiching a layer of the elastic pad. The deforming region is limited to one end of the fin ray (see Figure 4(d)). Multiple fin rays are arranged in parallel and connected by a fin membrane to achieve rajiform locomotion. Yan et al.⁷³ adopted a similar fin ray mechanism but used them in the pectoral fins of carangiform (see Figure 4(e)). Some basic gestures of the robotic pectoral fin, namely, relaxation, expansion, bending, cupping, and undulation, are realized by the SMA plates heated by resistance wire.

EAPs-based robotic fishes

EAP deforms when there is an electrical stimulus, which can be categorized into ionic EAPs and electronic EAPs. The ionic

polymer-metal composite (IPMC) and polypyrrole (PPy) based on ionic EAPs and the dielectric elastomer (DE) based on electronic EAPs are reported in robotic fish design.

When an electric field is applied to IPMC, it will cause its anions and cations to redistribute. The high concentration of cations on the cathode side will cause expansion effects, while the anode side is the opposite, and then the deformation of bending is produced.⁷⁴ IPMC has relatively small output stress (0.3 MPa) and low applied voltage (1~3 V),⁶³ which makes it suitable for small-sized robotic fish actuation (less than 100 mm in length^{75,76}). The designs of IPMC actuation share similarities. The flexible IPMC part is utilized as a flapper to oscillate the passive fins.^{77–79} Zheng et al.⁸⁰ developed a robotic manta ray and used the IPMC as a part of the wing-shaped pectoral fins, shaped like a trapezoid, and the rest remains to be passive. Hubbard et al.⁸¹ developed a special IPMC with a deformable surface, capable of realizing bending, twisting, and flapping motions. They used the designed IPMC as the pectoral fin and connected the IPMC to a caudal fin for

propulsion. Maneuvering motions, such as pitching, rolling, and yawing, are realized (see Figure 5(a)). Apart from the relatively low stress, the back-relaxation phenomenon, that is, the bending angle of IPMC increases in a certain time and then slowly decreases, is needed to be considered.⁸² It is verified that the peak angle value and the time to reach the peak are related to the water salinity and the applied voltage.⁸² The reason for this phenomenon is the entry of water from the outside to the inside of the IPMC.⁸³

The PPy actuator is fabricated by using electrochemical deposition to deposit PPy conductive polymer on both sides of polyvinylidene fluoride film to form a three-layer structure.⁸⁵ It will cause volume expansion to produce bending displacement when a small voltage is applied. This kind of actuator has the advantages of low cost, high conductivity, and fast response. McGovern et al.⁸⁶ described a method for measuring the thrust of a PPy actuator and studied the potential of the conductive polymer actuator as a robotic fish propulsion element by comparing the generated thrust with the synthetic speed of the robotic fish. A prototype⁸⁷ actuated by a PPy actuator reaches the maximum speed of 33 mm/s (0.25 BL/s) with a diameter of 20 mm.

For the DE actuator, when voltage is applied, the Maxwell stress is generated between the two electrodes and deforms the membrane in the thickness direction, resulting in area expansion.⁸⁸ DE possesses a fast response (less than 200 μ s) and a large actuation strain (over 100%), but the applied voltage is relatively high (over 1 kV).⁶⁵ In order to deal with insulation problems, Li et al.⁶⁴ found that the conductivity of the surrounding open water is weak but sufficient to serve as the ground electrode, while the hydrogel film sandwiched by two DE membranes is another electrode. The leading edges of the fins are rigid to lead to the undulatory motions of the entire fins when flapping (see Figure 5(b)). Li et al.⁶ developed a robot inspired by snailfish, which lives in the deep sea (see Figure 5(d)). The DE actuators are served as links between the fish body and fins. To adapt to the high pressure of the deep sea, they adopted a triblock copolymer, poly (styrene-*b*-butyl acrylate-*b*-styrene) in the DE actuator to increase the voltage-induced area strain. The robot succeeds in flapping for 45 min in the Mariana Trench (10900 m) and reaches a speed of 2.76 cm/s (0.24 BL/s) in the experimental condition of 110 MPa, which is a breakthrough in deep sea exploration. Shintake et al.⁸⁴ designed a prototype consisting of silicon substrate and elastomer membrane layers. They arranged the inside high-voltage electrodes smaller than other layers, making that there was no electrical short-circuit path through the water and thereby realizing the insulation (see Figure 5(c)). The swimming speed of the robot reaches a maximum of 37.2 mm/s (0.25 BL/s) with wired power.

PZT-based robotic fishes

The principle of PZT is based on the inverse piezoelectric effect, which results in structural deformation on electrical excitation. PZT actuators exhibit relatively high driving stress (about 110 MPa) and fast frequency, while the strain is relatively small (0.2%).²⁵ Typically, the robots actuated by PZT require a stroke magnification mechanism. Borgen et al.⁸⁹ used two THin-layer composite UNimorph ferroelectric DrivER and sensor (THUNDERS) (PZT actuator developed by Mossi et al.⁹⁰), respectively, connected to the tail fin. Although the magnifying mechanism is eliminated, the size of the actuator itself is large, which still makes the robotic fish bulky. The lightweight piezocomposite actuator (LIPCA), another PZT actuator, is superior to THUNDER in many aspects, but the driving displacement is still very small. Heo et al.⁹¹ adopted a rack-and-pinion system to amplify the displacement (see Figure 6(a)). Nguyen et al.⁹² used four layers of LIPCA connecting with a magnifying system to flap the fish tail (see Figure 6(b)). Zhao et al.⁹³ developed a micro-robotic fish (total mass: 1.93 g) with double caudal fins. The caudal fins are actuated by PZT bimorph cantilevers (36 mm, 2.1 mm, and 0.8 mm in length, width, and height, respectively) through a four-bar linkage transmission (see Figure 6(c)). The close or open movement is realized to improve the robotic stability and maneuverability when flapping. The maximum speed of the robot is about 4.5 cm/s (0.75 BL/s).

Macro fiber composite (MFC), another type of piezoelectric material, comprises rectangular cross-sectional piezoelectric fibers and interdigitated electrodes.⁹⁵ In addition to good flexibility and large driving force, MFC strikes a balance between the deformation and actuation force, which means that the additional magnifying mechanism is not required. Govindarajan et al.⁹⁶ tested the performance of the MFC flapping beam underwater. They observed that the beam reached its maximum efficiency of 55% at the frequency of 2.0 Hz and the maximum thrust reached 45 mN. Cen et al.⁹⁷ created the first prototype actuated by MFC. It is a conceptual model that the piezoelectric MFC bimorph actuator (without caudal fin) is connected to the main body. The robot reaches a swimming speed of 7.5 cm/s (0.3 BL/s), which shows the feasibility of the MFC-actuated robotic fish. In addition, Tan et al.⁹⁵ designed a modular MFC bimorph tail connected to the body. With the actuation of the MFC actuator, the prototype reaches the maximum speed of 0.25 m/s (0.8 BL/s). Hu et al.⁹⁴ attached two MFCs to the caudal fin-like substrate. The MFC is 20 mm in width and 29.6 mm in length (see Figure 6(d)). They carefully designed a thrust measurement system, and the maximum mean thrust of 2.95 mN was observed.

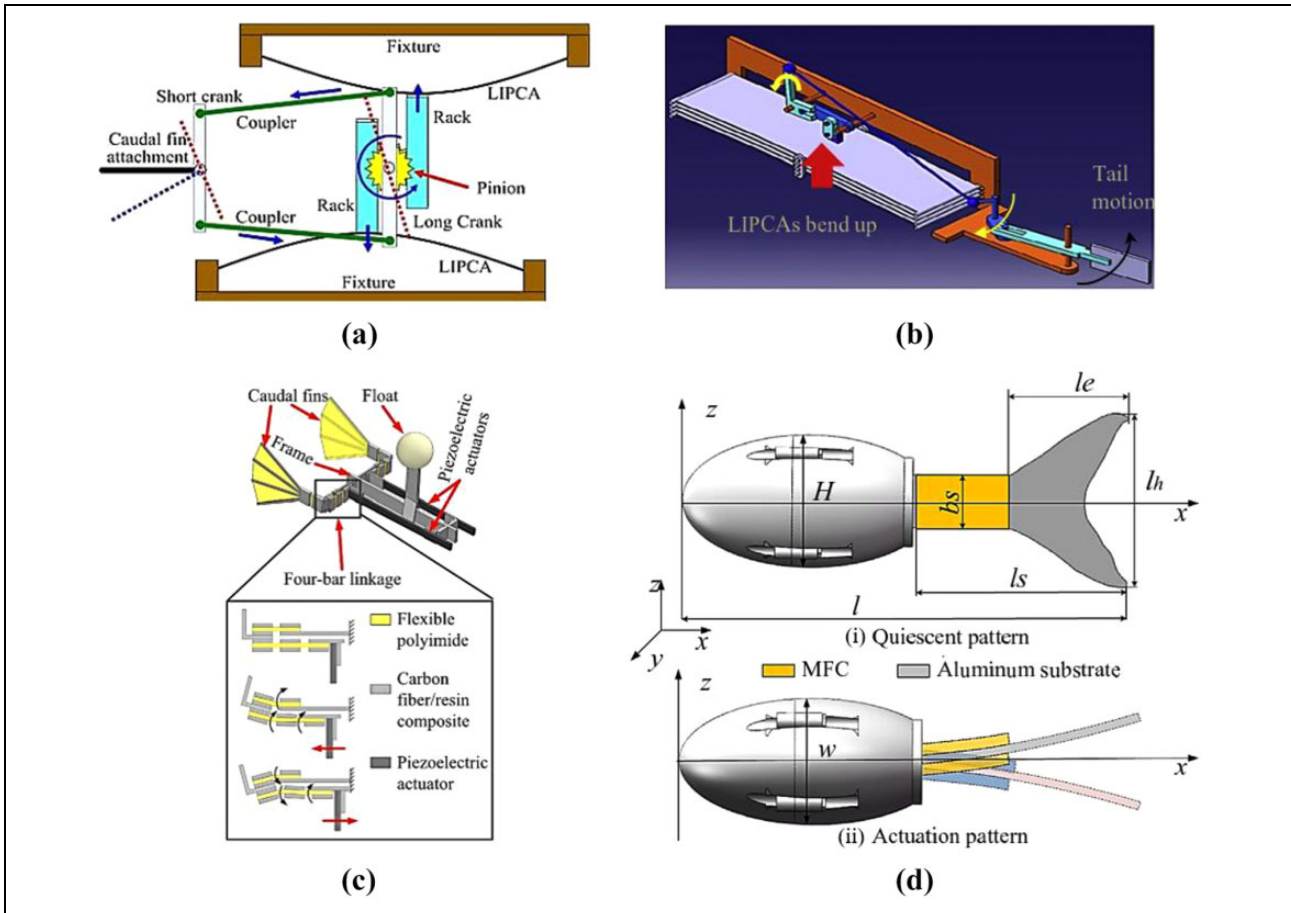


Figure 6. PZT-based robotic fishes: (a) The movement of LIPCA is transformed into the rotation of gears, which drives the rotation of the four-bar mechanism, thereby flapping the caudal fin. Reproduced with permission.⁹¹ Copyright 2021, Springer. (b) When LIPCAs bend up, the flapping tail motion is realized through the long link and vice versa. Reproduced with permission.⁹² Copyright 2010, IOP publishing. (c) Schematic of the micro-robotic fish and the movements of four-bar linkage transmission. Reproduced with permission.⁹³ Copyright 2021, Elsevier. (d) Structure diagram of the MFC-actuated bionic robotic fish. Reproduced with permission.⁹⁴ Copyright 2021, Academic Press-Elsevier Science. PZT: piezoelectric actuators; LIPCA: lightweight piezocomposite actuator; MFC: macro fiber composite.

FEA-based robotic fishes

FEA is integrated within and distributed throughout the body, which makes the robot soft and compliant.⁶⁶ FEA is made of super-elastic materials inside with several chambers expanded by pressurized gas or liquid, resulting in bending or stretching motion. Pneumatic and hydraulic actuators are two categories in underwater applications. Marchese et al.⁹⁸ developed a robotic fish that comprises two pairs of pneumatic layers longitudinally attached to an inextensible constraint layer (see Figure 7(a)). With an onboard gas regulation mechanism, the robot achieves escape maneuvers of a maximum heading angle of 100 degrees. However, the insufficient power supply resulting in limited endurance and the uncontrollable buoyancy center due to the release of gas are unignorable problems. In contrast, hydraulic actuators are capable of using surrounding water in a cycle, providing faster frequency response and larger force. Katzschmann et al.⁴ adopted a similar actuator structure but used an onboard gear bump to

pressure the fluid (see Figure 7(b)). The robot could dive up to 18 m and swim at the speed of 0.5 BL/s and show good integration into the marine environment.

Furthermore, Chen et al.⁹⁹ studied the relationship between the bending angle and the pressure of the fluid. They developed a flexible water hydraulic soft bending actuator (FWBA) for a fishtail as shown in Figure 7(c). The bending angle of FWBA is approximately 79.8 degrees with the water pressure of 18 KPa, and the bending angle drops to 56.5 degrees with the water pressure of 20 KPa when paired FWBAs are adopted to flap a caudal fin.

Sensors for robotic fishes

Sensing technology is an essential part of the robotic fish. It can sense changes in the surrounding environment to provide feedback control. Generally, in terms of realizing autonomous navigation, infrared sensors are mainly used in the detection of obstacles, effectively in planning routes, and avoiding obstacles. Pressure sensors are used for depth

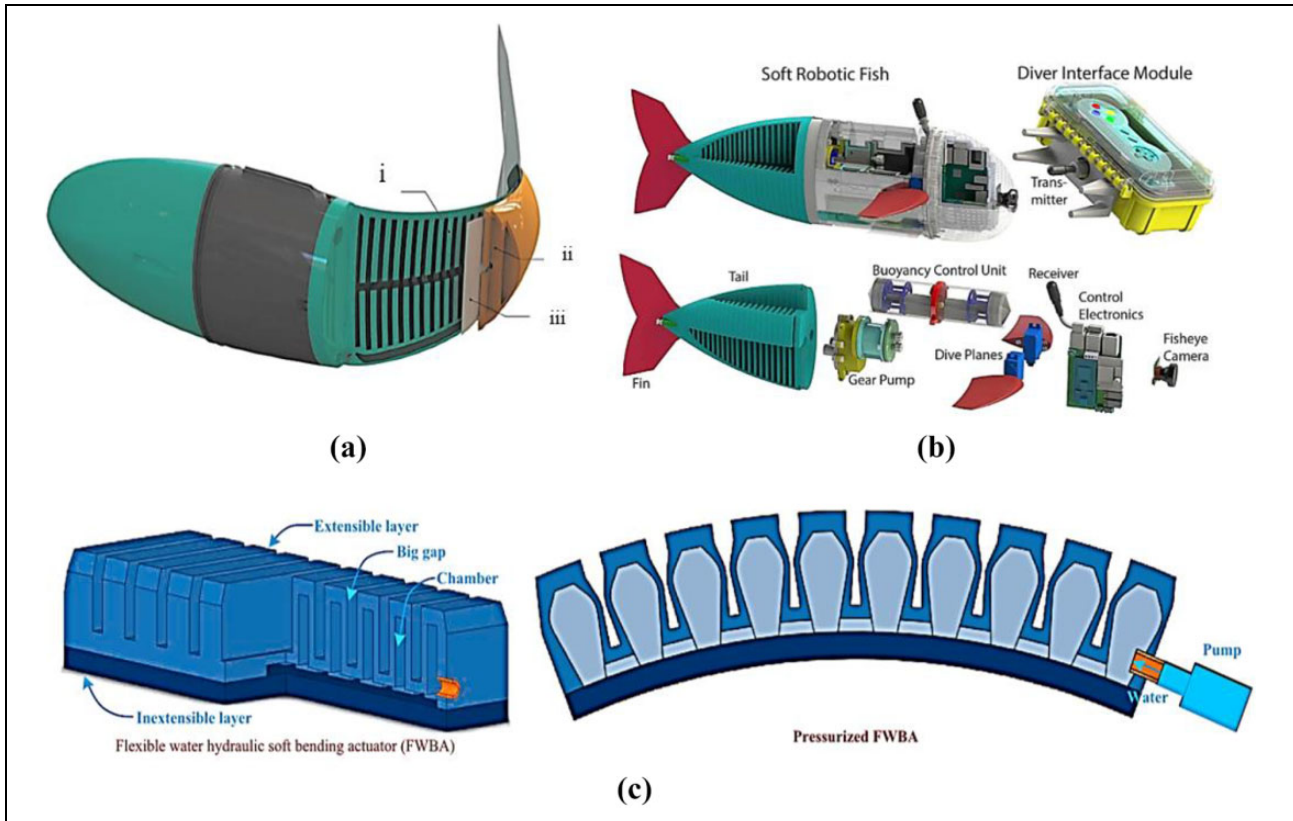


Figure 7. FEA-based robotic fishes: (a) (i) antagonistic actuator, (ii) flexible and inextensible layer, and (iii) agonistic actuator. Reproduced with permission.⁹⁸ Copyright 2014, Mary Ann Liebert. (b) Overview of Soft robotic fish (top right). The elastomer tail (cut view) is driven by a gear pump, and the two inlets at the tail form a liquid circulation. Dive planes are driven by servos to ascend or descend. The buoyancy control unit, control electronics including an acoustic receiver, and fisheye camera are the subcomponents of the system. Reproduced with permission.⁴ Copyright 2018, Amer Assoc Advancement Science. (c) Pre-stretched state (left) and the bending state of the FWBA (right). Reproduced with permission.⁹⁹ Copyright 2021, Elsevier Sci. FEA: fluid elastomer actuator; FWBA: flexible water hydraulic soft bending actuator.

perception to prevent excessive pressure from damaging components. Accelerometer and gyroscope are used to maintain the stable swimming of the robotic fish. Compass realizes the direction recognition. The current sensor predicts battery life and provides variable current to the robot. Force/torque sensor measures thrust. More details are presented in Table 4.

As an important part of underwater perception, artificial lateral line (ALL) has received more and more attention. The lateral line system is a unique skin sensory organ of aquatic vertebrates.¹¹⁹ The basic sensory unit of the lateral line is the neuroma, which is a receptor organ that consists of sensory hair cells and support cells covered by a gelatinous cupula.¹²⁰ The ALL system inspired by it uses pressure sensors as the main sensing components. Multiple pressure sensors are distributed on the surface of the fuselage. Specifically, Wang et al.¹²¹ distributed nine pressure sensors around the body to perceive the state of adjacent robotic fish by sensing the reverse Carmen vortex street. Zheng et al.¹²² distributed eleven pressure sensors on the fuselage: four at each side of the shell, one at the tip of the head, and two at the top and bottom of the head. The state

of adjacent fish was obtained by collecting hydrodynamic pressure variations data. Furthermore, piezoresistive, piezoelectric, capacitive, optical, and hot-wire sensors can be used to build ALL systems as well. See literature¹²³ for more details.

Modeling and control of robotic fishes

Modeling and control are considered to be the core parts of the robotic fish design. In this section, the methods of dynamic modeling are first presented. Then, two main control approaches: (1) trajectory approximation method and (2) central pattern generators (CPGs) are reviewed.

Dynamic modeling

Due to the complexity of the morphology and hydrodynamics of fish, it is very difficult to establish an accurate dynamic model. The numerical method and analytical method are typically adopted. The former often requires the establishment of N-S equations. Computational Fluid Dynamics (CFD) is applied to numerical simulations.

Table 4. Different types of sensors used in robotic fishes.

Sensor type	Sensor model	Applications
Camera	<ul style="list-style-type: none"> • CMOS camera^{100, 101} • CCD camera¹⁰² 	<ul style="list-style-type: none"> • Positioning and tracking¹⁰⁰
Infrared sensor	<ul style="list-style-type: none"> • Sharp GP2Y0A21YK0F¹⁰³ • GP2Y0A02YK(0 to 15 psi)¹⁰⁴ 	<ul style="list-style-type: none"> • Detect obstacles^{103, 105, 106} • Remote control receiver⁷⁵
Pressure sensor	<ul style="list-style-type: none"> • CYY4¹⁰⁷ • CPI31¹⁰⁸ • MS5803-01BA¹⁰⁹ • 40PC001¹¹⁰ • 40PC015¹⁰⁴ 	<ul style="list-style-type: none"> • Depth control^{101, 104, 105, 107, 110} • Remote control¹¹¹ • Estimate the speed of the underwater robot¹⁰⁸ • Control the orientation of the robot¹⁰⁹
Compass	<ul style="list-style-type: none"> • Dinsmore 1490 sensor¹¹² 	<ul style="list-style-type: none"> • Navigation¹¹²
Accelerometer	<ul style="list-style-type: none"> • ADXL330(6.78 mg)¹¹³ 	<ul style="list-style-type: none"> • Measure the static gravity acceleration¹¹³
Gyroscope	<ul style="list-style-type: none"> • LPR503AL, LPY503AL¹⁰⁰ • MPU9150¹⁰⁷ • IDG300(2.44 °/s)¹¹³ 	<ul style="list-style-type: none"> • Improve positioning accuracy¹⁰⁰ • 3D motion control¹⁰⁷ • Provide the angular rate¹¹³
Servo angle sensor	<ul style="list-style-type: none"> • MAE-3 US-Digital¹¹³ 	<ul style="list-style-type: none"> • Measure exact angular displacement¹¹³
Current sensor	<ul style="list-style-type: none"> • ACS712¹¹⁴ 	<ul style="list-style-type: none"> • Measure torque¹¹⁴
Soft eGaN sensor	<ul style="list-style-type: none"> • Not available 	<ul style="list-style-type: none"> • Curvature estimation¹¹⁵ • Strain sensing¹¹⁶ • Measure thrust¹¹⁷
Force/torque sensor	<ul style="list-style-type: none"> • Nano 17¹¹⁷ 	
Temperature sensor	<ul style="list-style-type: none"> • TC1047A⁴¹ 	<ul style="list-style-type: none"> • Detect water temperature¹¹⁸

Using the CFD method based on the N–S equations, the viscous force can be fully considered, and the unsteady and nonlinear effects caused by the tail swing can be analyzed, which makes the hydrodynamic prediction more reliable.¹²⁴ However, this method is very time-consuming due to the huge amounts of calculations, and it lacks the support of classified and fined experimental data. The latter, based on certain simplifications, is more feasible but less accurate. For instance, the Resistive Force Theory¹³ is only suitable in the low Reynolds number condition for neglecting the inertia force. The WPT¹⁵ simplifies the fish body as a flexible thin plate for wave motion, thereby being more suitable for the flatfish swimming. The EBT¹⁴ is suitable for slender fish with small lateral deformation. It presents that the thrust of the fish is generated by the additional momentum corresponding to the motion of the fish body wave propagating backward. Based on the momentum balance in the hemisphere control volume containing the fish body, the effect of wake dynamics is also approximated. The large-amplitude elongated-body theory¹⁸ proposed later extends its applications to larger lateral deformation, which makes it the most acceptable theory. In addition, Yu et al.¹²⁵ proposed a data-driven approach. In their method, the dynamic model is first derived with the Morrison

equation and the strip method, and the parameters are directly identified from experimental data and integrated into the dynamic model to reshape it. Therefore, it is applicable to model swimming robots with complex and irregular geometric profiles and numerous heterogeneous hydrodynamic parameters.

Trajectory approximation

To approximate the trajectories of the fishes, it is important to get a deep understanding of the principles of their locomotion, which is characterized by the deforming bodies. A widely adopted function of the traveling body wave is proposed by Lighthill¹⁴

$$y_{body}(x, t) = [(c_1x + c_2x^2)][\sin(kx + wt)] \quad (1)$$

where y_{body} denotes the lateral displacement of the fish, x denotes the displacement along the fish axis, $k = 2\pi/\lambda$, λ denotes the wavelength, w denotes the body wave frequency, c_1 denotes linear wave amplitude envelope, and c_2 denotes quadratic wave amplitude envelope. To eliminate the head swing of fish for stable swimming, the new function is obtained by subtracting the function of the head from the traveling wave function above.¹²⁶ The

head is typically considered to be rigid, thus the function is linear

$$y_{\text{head}}(x, t) = c_3 x = \frac{\partial y_{\text{body}}(x, t)}{\partial x} \Big|_{x=0} = c_1 x \sin(\omega t) \quad (2)$$

where $y_{\text{head}}(x, t)$ denotes the lateral displacement of the head and c_3 denotes the coefficient of the linear equation of the head. The redefined lateral displacement of the fish, $y_{\text{BODY}}(x, t)$, is obtained

$$\begin{aligned} y_{\text{BODY}}(x, t) &= y_{\text{body}}(x, t) - y_{\text{head}}(x, t) \\ &= (c_1 x + c_2 x^2) \sin(kx + \omega t) - c_1 x \sin(\omega t) \end{aligned} \quad (3)$$

Then, the function is discretized to fitting the body wave

$$\begin{aligned} y_{\text{BODY}}(x, t) &= (c_1 x + c_2 x^2) \sin\left(kx - \frac{2\pi}{M} i\right) \\ &\quad - c_1 x \sin\left(-\frac{2\pi}{M} i\right), i \in [0, M - 1] \end{aligned} \quad (4)$$

where i is a serial number in an undulation circle and M represents the resolution of the discrete travelling wave. Therefore, a $M \times N$ look-up table of the joints is obtained (N denotes the number of joints).

Similarly, other swimming patterns could be realized by establishing corresponding kinematic functions.¹²⁷ In conclusion, this method is easy to implement but could not realize smooth gait transition, and the instantaneous torque changes and jerky movements have the risk of damaging the motors and gearboxes. Moreover, the online parameter tuning is difficult since each joint involves many values to promise accuracy.

Central pattern generator

Another control method is to use CPG, which is a neural network that exists in both invertebrates and vertebrates. It can generate rhythmic neural activity patterns, such as respiration, chewing, and sucking, in the absence of external signal input like sensory feedback or higher control centers.¹²⁸ In biology, CPG is turned out to be a distributed network composed of several coupled oscillators, which is suitable for multi-link mechanisms.¹²⁹ In particular, the oscillators are coupled in a certain topology, and each of the oscillators is in charge of a specific joint. Simple or low-dimensional input signals are sufficient to propose the coordinated wave motion of the robot. CPG-based controller exhibits superiorities: (1) provides stable rhythmic patterns, (2) realizes diverse motion modes of the robot through a variety of stable phase relationships, (3) presents smooth transition online between different gaits with simple control parameters, and (4) although CPG does not require sensory feedback, they are crucial to shaping the CPG control to improve adaptability and robustness.

CPG models. The first step to construct a CPG controller is to choose an appropriate CPG control model. The most

widely used CPG model in a robotic fish domain is the oscillator model, of which the most common are the Hopf oscillator and the Ijspeert phase oscillator.

Hopf oscillator possesses a stable limit cycle.¹³⁰ It is able to produce sinusoidal oscillation independently. The dynamics of the Hopf oscillator could be described by the following differential equations

$$\begin{aligned} \dot{x} &= (\mu^2 - (x^2 + y^2))x + \omega y \\ \dot{y} &= (\mu^2 - (x^2 + y^2))y - \omega x \end{aligned} \quad (5)$$

where x and y are the states of the oscillator, ω is the intrinsic oscillation frequency, and μ determines the steady-state amplitude of oscillation, that is, the state variables x and y will eventually converge to a stable limit cycle with μ as the radius. It should be noted that there are no parameters to control the phase lags. Actually, the phase lags are determined by the coupling weight between the joints and added as an extra term to the equations.

Ijspeert et al.¹³¹ developed a phase oscillator to control a salamander robot. The oscillator could be described as follows

$$\begin{aligned} \dot{\theta}_i &= 2\pi v_i + \sum_j r_j w_{ij} \sin(\theta_j - \theta_i - \phi_{ij}) \\ \ddot{r}_i &= a_i \left(\frac{a_i}{4} (R_i - r_i) - \dot{r}_i \right) \\ x_i &= r_i \left(1 + \cos(\theta_i) \right) \end{aligned} \quad (6)$$

where θ_i and r_i are the state variables representing the phase and the amplitude of oscillator i , v_i and R_i determine its intrinsic frequency and amplitude, and a_i denotes the amplitude convergence speed. Couplings between oscillators are defined by the weights w_{ij} and phase biases ϕ_{ij} . A positive oscillatory signal, x_i , represents the output of oscillator i . The phase model is an abstract simulation of the biological movement process. The system also exhibits limit cycle behavior, and the analytical solution clearly expresses the parameters controlling amplitude, frequency, and phase lag.

Parameter tuning. Parameter tuning is the key problem in CPG modulation, as the CPGs involve many uncertain parameters in the equations while a well-established design methodology for CPGs to achieve the desired motion behavior is still missing. Lately, some intelligent learning methods are being proposed. Yu et al.¹³² searched the optimized parameters by integrating particle swarm optimization (PSO) and a dynamic model. In PSO, each particle has the ability to perceive the best position of itself and the swarm and then adjust its actions based on this information by iteration. Specifically, the dynamic model is first developed as a guide to search the control parameters and the

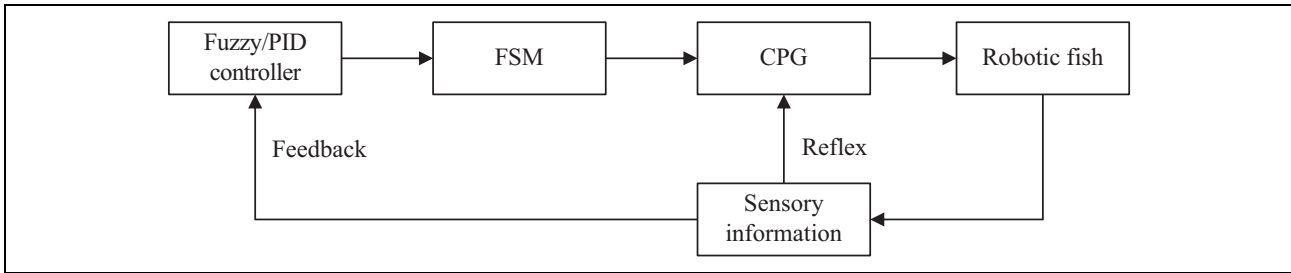


Figure 8. The schematic of the close-loop CPG system. CPG: central pattern generator.

swimming patterns, and then, the PSO refines the searched parameters of the CPGs. Zhou et al.¹³³ adopted the genetic algorithm (GA) to optimize the parameters of the CPGs as GA possesses high-dimensional global searching capability. The speed and the instantaneous swimming power consumption are used as feedback to improve the controlling parameters by GA. Hu et al.¹³⁴ proposed a learning method to acquire fishlike swimming. First, they used the trajectory approximation method to obtain the joint angles as the teaching signals. By converting the parameters of frequency, phase difference, and amplitude into new state variables with their own dynamics, the teaching signals and their phase relations could be learned by the CPG network, thus the instructed locomotor pattern can be reproduced by the robotic fish. The learning is embedded into the dynamics of the oscillator, thereby external optimization or preprocessing of the teaching signal is not required. Ren et al.¹³⁵ proposed a general internal model (GIM)-based learning method. The GIM is composed of three components, namely the inner Hopf oscillator, the artificial neural network (ANN), and the outer signal modulator. The Hopf oscillator generates periodic input signals. The ANN is trained to yield the desired motion patterns when receiving the input signals from the inner Hopf oscillator, and the outer signal modulator adjusts the amplitude of the generated motion pattern according to task specifications since the output of the ANN cannot be resized by the input as the ANN is a nonlinear mapping. The GIM exhibits excellent function approximation ability, and the speed and direction control are realized by monotonically tuning parameters.

Close-loop CPG system. The close-loop CPG system plays a very significant role in the generation of diverse and stable movements. The framework of closed-loop control is schematically shown in Figure 8. Specifically, the sensory signal generated by them could directly act on the CPG, like a reflex action, which is an involuntary and nearly instantaneous movement in response to a stimulus, or received by the high-level center as feedback. Due to the nonlinear environment, the fuzzy or (proportional–integral–derivative) controller is adopted as the high-level center to decide the swimming mode based on the feedback. The gait transition could be realized by a finite state machine (FSM)

since each gait corresponds to a set of control parameters. The combination of the CPGs and the FSM provides an effective way to switch locomotor patterns. Under this frame, Bal et al.¹³⁶ realized excellent autonomous swimming performance through precise yaw control. Yan et al.¹³⁷ achieved stable motion mode switching between swimming and crawling.

Challenges and future directions

With the unique driving characteristics and application diversity, robotic fish will certainly become one of the major development trends in performing underwater tasks. However, there is a gap between the robotic fish and the real fish regarding the performance. The maximum speed of the robotic fish is 3.7 m/s, which is far more outstanding than others, while the swordfish reaches about 27 m/s. The maximum turning speed of the robotic fish is 670 °/s, while the archerfish is 4500 °/s. Moreover, fishes exhibit flexible and freely maneuvering, such as escape, rapid acceleration, and braking, while the robotic fish only execute simple turning or diving. The possible directions of robotic fish might focus on the following aspects.

First, one possible direction is drag reduction, which might contribute to the high speed of real fish inspired by Gray's paradox.¹² The micron-scale caves distributed on the fish surface play an important role in drag reduction.¹³⁸ The concave shape creates a negative pressure area, sucking oil out of the hole to lubricate the surface to minimize frictional resistance. Dou et al.¹³⁹ developed a coating technology that autonomously forms the micron-scale caves when swimming. The gas-phase develops in the solid–liquid interface in low-pressure conditions due to flow separation and vortex and partially replaces the solid–liquid shear force with gas–liquid shear force, resulting in drag reduction. It is noteworthy that the drag reduction efficiency of the bionic surface becomes more significant as the flow rate increases (over 10% at the flow speed of 13.1 m/s). In the future, the drag reduction mechanism needs to be clarified, and more remarkable performance and simple fabrication of drag reduction technology are needed to be adopted in the robotic fish system.

Second, the question of improving the actuation system is another direction. On the one hand, the prototypes based

on the multi-link mechanism actuated by the traditional DC and servo motors still represent the state-of-the-art swimming speed. However, it cannot perfectly fit the flexible movement of real fish, and the friction loss caused by additional transmission mechanisms cannot be ignored. Furthermore, it requires multiple motors to independently drive the fin rib to reproduce the undulation of ribbon fins, which is bulky and difficult to control. The design of MAR, using a single helix to realize undulation, shows a new direction of actuation system simplification.³⁴ On the other hand, the smart materials and soft actuators can be well integrated into the body of the robot fish with a smaller size and higher maneuverability, but most of the robotic fish with such actuators have a maximum speed of no more than 3 BL/s.³¹ The FEA shows high compliance and the best “biomimicry”. This actuator is essentially powered by motors but uses fluid as the energy conversion medium, which gives it the advantages of high speed and flexible movement, especially the form of hydraulic exhibits great promise in terms of stability and energy recyclability. In the future, it is expected to be applied to undulation and muscle-like movements.

Third, the underwater perception is still not well-developed. Powerful perception offers detailed feedback in control and improves the adaptability of the robotic fish. However, current sensors, such as cameras, IMU, and GPS, have difficulty performing well in the harsh underwater environment. Moreover, they could only provide a single sensing signal and had blind areas, where they unable to sense objects or creatures’ subtle movements.¹⁴⁰ Lateral line is an important modality to sense the subtle changes in the water flow, which is composed of a row of neuromasts distributed throughout the fish body.¹²⁰ Based on it, the ALL is typically constructed by an array of distributed pressure sensors to sense the fluid velocity or reverse carmen vortex street, which is crucial to the perception among groups of underwater robots.¹⁴¹ However, it is still worth exploring how to realize real-world perception. Recently, the increasing interest in proprioceptive sensing provides a new direction for underwater perception, which utilizes the kinematics or parts of the body to extract useful information inflow.¹⁴² Since related research studies are just beginning, future directions might include determining the type of proprioceptive signal perceived and clarifying the neurotransmission mechanisms between proprioceptive and motor control.¹⁴³ From a long-term perspective, it is exciting to combine proprioceptive sensing with an ALL to realize powerful underwater perception.

Fourth, the control methods are needed to be improved. The close-loop CPG system has strong adaptability and robustness. However, how exactly the properties of sensory information affect the characteristics of the CPG output has not been fully investigated. Recent studies have shown that sensory feedback topology has a significant impact on the way that the neural oscillator setting affects the entrainment characteristics of the coupled system.¹⁴⁴ In general, a

systematic design method for sensory feedback control is needed to be developed in the future. Alternatively, considering the complexity of nonlinear hydrodynamics, the iterative learning control could be regarded as a potential candidate.¹⁴⁵ The accurate model is not required when an appropriate learning gain is chosen. The learning formulates the input signal based on previous experimental data, and good speed tracking performance is achieved with constant iteration during the entire operation interval. In the future, it is expected to be applied in tracking maneuvering movements, such as turning, yawing, or pitching motions.

Conclusions

In this article, we have reviewed the characteristics of different fish locomotion and the robot designs based on it. We also have outlined features of smart soft actuators and sensors. Then, we have summarized modeling and control methods for efficient and stable swimming. Fish have many complex structural features, most of which are not yet known clearly for their potential impact on swimming performance. However, it is certain that the use of mechanical devices for imitation is a sure way to help us understand the hydrodynamic principles of fish movement and thus achieve the transcendence of the real fish. The robotic fish is still in the preliminary prototype development stage, and there is still a certain distance from the practical application, but with its excellent potential performance, it will certainly expand a wide range of applications in military and civil applications.

Acknowledgments

This work was supported by the Zhejiang Provincial Natural Science Foundation of China (Grant Nos. LY22E050019 and GG21E050044) and the National Natural Science Foundation of China (Grant Nos. 51805482 and 51975523).


Declaration of conflicting interests

The author(s) declared no potential conflicts of interest with respect to the research, authorship, and/or publication of this article.

Funding

The author(s) disclosed receipt of the following financial support for the research, authorship, and/or publication of this article: This research is funded by natural science foundation of zhejiang province (GG21E050044 and LY22E050019) and national natural science foundation of china (51805482 and 51975523).

ORCID iD

Yi Li  <https://orcid.org/0000-0001-8485-2937>

References

1. Lauder GV. Fish locomotion: recent advances and new directions. *Ann Rev Mar Sci* 2015; 7: 521–545. 2014/09/25. DOI: 10.1146/annurev-marine-010814-015614.

2. Wen L, Wang TM, Wu GH, et al. Quantitative thrust efficiency of a self-propulsive robotic fish: experimental method and hydrodynamic investigation. *IEEE-ASME Transact Mechatron* 2013; 18: 1027–1038. Article. DOI: 10.1109/tmech.2012.2194719.
3. Reddy NS, Sen S, Shome SN, et al. An investigation on the performance of an oscillating flat plate fin with compliant joint for underwater robotic actuation. In: *1st IEEE international conference on control, measurement and instrumentation (CMI)*, Jadavpur Univ, Kolkata, INDIA, 08–10 January 2016, pp. 201–205. New York: IEEE.
4. Katzschmann RK, DelPreto J, MacCurdy R, et al. Exploration of underwater life with an acoustically controlled soft robotic fish. *Sci Robot* 2018; 3. 2018/03/21. DOI: 10.1126/scirobotics.aar3449.
5. Liang J, Wang T, and Wen L. Development of a two-joint robotic fish for real-world exploration. *J Field Robot* 2011; 28: 70–79. DOI: 10.1002/rob.20363.
6. Li GR, Chen XP, Zhou FH, et al. Self-powered soft robot in the Mariana Trench. *Nature* 2021; 591: 66–71. DOI: 10.1038/s41586-020-03153-z.
7. Zhang F, Ennasr O, Litchman E, et al. Autonomous sampling of water columns using gliding robotic fish: algorithms and harmful-algae-sampling experiments. *IEEE Syst J* 2016; 10: 1271–1281. DOI: 10.1109/jsyst.2015.2458173.
8. Zhang FT, Wang JX, Thon J, et al. Gliding robotic fish for mobile sampling of aquatic environments. In: *IEEE 11th international conference on networking, sensing and control (ICNSC)*, Miami, FL, 07–09 April 2014, pp.167–172. New York: IEEE.
9. Fattah SA, Abedin F, Ansary MN, et al. R3Diver: remote robotic rescue diver for rapid underwater search and rescue operation. In: *IEEE region 10 conference (TENCON)*, Singapore, 22–25 November 2016, pp. 3280–3283. New York: IEEE.
10. Wu Z, Liu J, Yu J, et al. Development of a novel robotic dolphin and its application to water quality monitoring. *IEEE/ASME Transact Mechatron* 2017; 22: 2130–2140. DOI: 10.1109/tmech.2017.2722009.
11. Breder CM. The locomotion of fishes. *Zoologica* 1926; 4: 159–256.
12. Gray J. Studies in animal locomotion, VI. The propulsive powers of the dolphin. *J Exp Biol* 1936; 13: 192–199.
13. Taylor G. Analysis of the swimming of long and narrow animals. *Proceed Royal Soc London* 1952; 214: 158–183.
14. Lighthill MJ. Note on the swimming of slender fish. *J Fluid Mechan* 1960; 9: 305–317. DOI: 10.1017/s002211206001110.
15. Wu YT. Swimming of a waving plate. *J Fluid Mechan* 1961; 10: 321–344. Article. DOI: 10.1017/S0022112061000949.
16. Cheng JY, Zhuang LX, and Tong BG. Analysis of swimming three-dimensional waving plates. *J Fluid Mechan* 1991; 232: 341–355. Article. DOI: 10.1017/S0022112091003713.
17. Horlock JH. Actuator disk theory. *McGraw-Hill International Book Company* 1978; 85: 29.
18. Lighthill M J. Large-amplitude elongated-body theory of fish locomotion. *Proceed Royal Soci London* 1971; 179: 125–138.
19. Triantafyllou MS and Triantafyllou GS. An efficient swimming machine. *Sci Am* 1995; 272: 64–70. DOI: 10.1038/scientificamerican0395-64.
20. Laschi C, Mazzolai B, and Cianchetti M. Soft robotics: technologies and systems pushing the boundaries of robot abilities. *Sci Robot* 2016; 1. 2016/12/06. DOI: 10.1126/scirobotics.aah3690.
21. Jin-Dong L and Huosheng H. Biologically inspired behaviour design for autonomous robotic fish. *Int J Automat Comput* 2006; 04: 16–27.
22. Zhou C and Low KH. Design and locomotion control of a biomimetic underwater vehicle with fin propulsion. *IEEE/ASME Transact Mechatron* 2012; 17: 25–35.
23. Zhang S, Qian Y, Liao P, et al. Design and control of an agile robotic fish with integrative biomimetic mechanisms. *IEEE/ASME Transact Mechatron* 2016; 21: 1846–1857.
24. Yu J, Ding R, Yang Q, et al. On a bio-inspired amphibious robot capable of multimodal motion. *IEEE-ASME Transact Mechatron* 2012; 17: 847–856.
25. Chu W-S, Lee K-T, Song S-H, et al. Review of biomimetic underwater robots using smart actuators. *Int J Precis Eng Manufact* 2012; 13: 1281–1292. DOI: 10.1007/s12541-012-0171-7.
26. Yu J, Ming W, Dong H, et al. Motion control and motion coordination of bionic robotic fish: a review. *J Bionic Eng* 2018; 15: 579–598.
27. Salazar R, Campos A, Fuentes V, et al. A review on the modeling, materials, and actuators of aquatic unmanned vehicles. *Ocean Eng* 2019; 172: 257–285.
28. Junzhi YU, Wen L, and Ren ZY. A survey on fabrication, control, and hydrodynamic function of biomimetic robotic fish. *Sci China Technol Sci* 2017; 60: 1–16.
29. Scaradozzi D, Palmieri G, Costa D, et al. BCF swimming locomotion for autonomous underwater robots: a review and a novel solution to improve control and efficiency. *Ocean Eng* 2017; 130: 437–453.
30. Raj A and Thakur A. Fish-inspired robots: design, sensing, actuation, and autonomy—a review of research. *Bioinsp Biomimet* 2016; 11: 031001.
31. Xie F, Zuo Q, Chen Q, et al. Designs of the biomimetic robotic fishes performing body and/or caudal fin (BCF) swimming locomotion: A review. *J Intell Robot Syst* 2021; 102: 1–19.
32. Sfakiotakis M, Lane DM, and Davies JBC. Review of fish swimming modes for aquatic locomotion. *IEEE J Oceanic Eng* 1999; 24: 237–252. DOI: 10.1109/48.757275.
33. Bayat B, Crespi A, Ijspeert A, et al. Envirobot: a bio-inspired environmental monitoring platform. In: *IEEE OES joint symposium/workshop on autonomous underwater vehicles (AUV)*, Univ Tokyo, Inst Ind Sci, Tokyo, Japan, 06–09 November 2016, pp. 381–386. New York: IEEE.
34. Struebig K, Bayat B, Eckert P, et al. Design and development of the efficient anguilliform swimming robot- MAR.

- Bioinspir Biomim* 2020; 15: 035001. 2020/01/16. DOI: 10.1088/1748-3190/ab6be0.
35. Clapham RJ and Hu H. *iSplash-II: Realizing fast carangiform swimming to outperform a real fish*. Berlin: Springer Berlin Heidelberg 2015.
 36. Zhong Y, Li Z, and Du RX. A novel robot fish with wire-driven active body and compliant tail. *IEEE-ASME Transact Mechatron* 2017; 22: 1633–1643. Article. DOI: 10.1109/tmech.2017.2712820.
 37. Algarin-Pinto JA, Garza-Castanon LE, Vargas-Martinez A, et al. Dynamic modeling and control of a parallel mechanism used in the propulsion system of a biomimetic underwater vehicle. *Appl Sci-Basel* 2021; 11. DOI: 10.3390/app1114909.
 38. Costa D, Palmieri G, Palpacelli MC, et al. Design of a bio-inspired autonomous underwater robot. *J Intell Robot Syst* 2018; 91: 181–192. Article. DOI: 10.1007/s10846-017-0678-3.
 39. Zhang R, Shen Z, and Wang Z. Ostraciiform underwater robot with segmented caudal fin. *IEEE Robot Autom Lett* 2018; 3: 2902–2909. DOI: 10.1109/lra.2018.2847198.
 40. Zhou CL and Low KH. Design and locomotion control of a biomimetic underwater vehicle with fin propulsion. *IEEE-ASME Transact Mechatron* 2012; 17: 25–35. DOI: 10.1109/tmech.2011.2175004.
 41. Cai Y, Bi S, Li G, et al. From natural complexity to biomimetic simplification the realization of bionic fish inspired by the cownose ray. *IEEE Robot Automat Magaz* 2019; 26: 27–38. DOI: 10.1109/mra.2018.2861985.
 42. Park S-J, Gazzola M, Park KS, et al. Phototactic guidance of a tissue-engineered soft-robotic ray. *Science* 2016; 353: 158–162. DOI: 10.1126/science.aaf4292.
 43. Hu T, Shen L, Lin L, et al. Biological inspirations, kinematics modeling, mechanism design and experiments on an undulating robotic fin inspired by *Gymnarchus niloticus*. *Mechan Mach Theory* 2009; 44: 633–645. DOI: 10.1016/j.mechmachtheory.2008.08.013.
 44. Curet OM, Patankar NA, Lauder GV, et al. Aquatic manoeuvring with counter-propagating waves: a novel locomotive strategy. *J Royal Soc Inter* 2011; 8: 1041–1050. DOI: 10.1098/rsif.2010.0493.
 45. Liu H and Curet O. Swimming performance of a bio-inspired robotic vessel with undulating fin propulsion. *Bioinspirat Biomimet* 2018; 13. DOI: 10.1088/1748-3190/aacd26.
 46. Liu F, Lee K-M, and Yang C-J. Hydrodynamics of an undulating fin for a wave-like locomotion system design. *IEEE-ASME Transact Mechatr* 2012; 17: 554–562. DOI: 10.1109/tmech.2011.2107747.
 47. Behbahani SB and Tan X. Bio-inspired flexible joints with passive feathering for robotic fish pectoral fins. *Bioinspirat Biomimet* 2016; 11. DOI: 10.1088/1748-3190/11/3/036009.
 48. Pham VA, Nguyen TT, Lee BR, et al. Dynamic analysis of a robotic fish propelled by flexible folding pectoral fins. *Robotica* 2020; 38: 699–718. DOI: 10.1017/s0263574719000997.
 49. Gray J. Studies in animal locomotion. *J Exp Biol* 1933; 10: 88–104. DOI: 10.1242/jeb.10.1.88.
 50. Duraisamy P, Sidharthan RK, and Santhanakrishnan MN. Design, modeling, and control of biomimetic fish robot: a review. *J Bionic Eng* 2019; 16: 967–993. DOI: 10.1007/s42235-019-0111-7.
 51. Raj A and Thakur A. Fish-inspired robots: design, sensing, actuation, and autonomy—a review of research. *Bioinspir Biomimet* 2016; 11. DOI: 10.1088/1748-3190/11/3/031001.
 52. Yu JZ, Tan M, Wang S, et al. Development of a biomimetic robotic fish and its control algorithm. *IEEE Transact Syst Man Cybernet Part B-Cybernet* 2004; 34: 1798–1810. DOI: 10.1109/tsmcb.2004.831151.
 53. Yu J, Ding R, Yang Q, et al. Amphibious pattern design of a robotic fish with wheel-propeller-fin mechanisms. *J Field Robot* 2013; 30: 702–716.
 54. Yu J, Kai W, Min T, et al. Design and control of an embedded vision guided robotic fish with multiple control surfaces. *Scient World J* 2014; 2014: 631296.
 55. Hu Y, Liang J, and Wang T. Mechatronic design and locomotion control of a robotic thunniform swimmer for fast cruising. *Bioinspir Biomim* 2015; 10: 026006. 2015/03/31. DOI: 10.1088/1748-3190/10/2/026006.
 56. Kodati P, Hinkle J, Winn A, et al. Microautonomous robotic ostraciiform (MARCO): hydrodynamics, design, and fabrication. *IEEE Transact Robot* 2008; 24: 105–117. DOI: 10.1109/tro.2008.915446.
 57. Salazar R, Fuentes V, and Abdelkefi A. Classification of biological and bioinspired aquatic systems: a review. *Ocean Eng* 2018; 148: 75–114. DOI: 10.1016/j.oceaneng.2017.11.012.
 58. Jagnandan K and Sanford CP. Kinematics of ribbon-fin locomotion in the bowfin, *amia calva*. *J Exper Zool Part A-Ecol Integrat Phys* 2013; 319: 569–583. DOI: 10.1002/jez.1819.
 59. Oufiero CE, Kraskura K, Bennington R, et al. Individual repeatability of locomotor kinematics and swimming performance in a gymnotiform swimmer. *Physiol Biochem Zool* 2021; 94: 22–34. DOI: 10.1086/712058.
 60. Sitorus PE, Nazaruddin YY, Leksono E, et al. Design and implementation of paired pectoral fins locomotion of labriform fish applied to a fish robot. *J Bionic Eng* 2009; 6: 37–45. DOI: 10.1016/s1672-6529(08)60100-6.
 61. Josie H, Utku C, Fabio G, et al. Soft manipulators and grippers: a review. *Front Robot AI* 2016; 3: 69.
 62. Hunter IW and Lafontaine S. A comparison of muscle with artificial actuators. *Technical Digest IEEE Solid-State Sensor and Actuator Workshop (Cat No92TH0403-X)* 1992: 178–185. Conference Paper. DOI: 10.1109/solsen.1992.228297.
 63. Bhandari B, Lee G-Y, and Ahn S-H. A review on IPMC material as actuators and sensors: fabrications, characteristics and applications. *Int J Precis Eng Manuf* 2012; 13: 141–163. DOI: 10.1007/s12541-012-0020-8.
 64. Li T, Li G, Liang Y, et al. Fast-moving soft electronic fish. *Sci Adv* 2017; 3. DOI: 10.1126/sciadv.1602045.
 65. O'Halloran A, O'Malley F, and McHugh P. A review on dielectric elastomer actuators, technology, applications, and

- challenges. *J Appl Phys* 2008; 104: 9. DOI: 10.1063/1.2981642.
66. Katzschmann RK, Marchese AD, and Rus D. Hydraulic autonomous soft robotic fish for 3D swimming. In: *14th International symposium on experimental robotics (ISER)* Morocco, 15–18 June 2014, pp. 405–420. Cham: Springer International Publishing Ag.
 67. Huang XN, Michael F, Patterson ZJ, et al. Shape memory materials for electrically-powered soft machines. *J Mat Chem B* 2020; 8: 4539–4551. Review. DOI: 10.1039/d0tb00392a.
 68. Huang XN, Kumar K, Jawed MK, et al. Highly dynamic shape memory alloy actuator for fast moving soft robots. *Adv Mater Technol* 2019; 4: 9. Article. DOI: 10.1002/admt.201800540.
 69. Li J, He JM, Wang YW, et al. A biomimetic flexible fishtail embedded with shape memory alloy wires. *IEEE Access* 2019; 7: 166906–166916. Article. DOI: 10.1109/access.2019.2953546.
 70. Coral W, Rossi C, Curet OM, et al. Design and assessment of a flexible fish robot actuated by shape memory alloys. *Bioinspir Biomim* 2018; 13: 056009. 2018/07/04. DOI: 10.1088/1748-3190/aad0ae.
 71. Cho KJ, Hawkes E, Quinn C, et al. Design, fabrication and analysis of a body-caudal fin propulsion system for a micro-robotic fish. In: *IEEE international conference on robotics and automation*, Pasadena, CA, 19–23 May 2008, vols 1–9, pp. 706–711. New York: IEEE.
 72. Zhang YH, He JH, and Low K. Design and motion testing of a multiple SMA fin driven BIUV. *J Hydrodyn* 2019; 31: 124–136. Article. DOI: 10.1007/s42241-018-0148-9.
 73. Yan Q, Wang L, Liu B, et al. A novel implementation of a flexible robotic fin actuated by shape memory alloy. *J Bionic Eng* 2012; 9: 156–165. DOI: 10.1016/s1672-6529(11)60111-x.
 74. Chen Z. A review on robotic fish enabled by ionic polymer-metal composite artificial muscles. *Robotics Biomim* 2017; 4: 24. 2017/12/22. DOI: 10.1186/s40638-017-0081-3.
 75. Ye XF, Su YD, Guo SX, et al. A centimeter-scale autonomous robotic fish actuated by IPMC actuator. In: *IEEE international conference on robotics and biomimetics (ROBIO 2007)*, Sanya, Peoples R China, 15–18 December 2007, vols 1–5, pp. 262–267. New York: IEEE.
 76. Shen Q, Wang TM, Liang JH, et al. Hydrodynamic performance of a biomimetic robotic swimmer actuated by ionic polymer-metal composite. *Smart Mater Struct* 2013; 22: 13. Article. DOI: 10.1088/0964-1726/22/7/075035.
 77. Aureli M, Kopman V, and Porfiri M. Free-locomotion of underwater vehicles actuated by ionic polymer metal composites. *IEEE/ASME Transact Mechatron* 2010; 15: 603–614. DOI: 10.1109/tmech.2009.2030887.
 78. Zheng C, Shatara S, and Xiaobo T. Modeling of biomimetic robotic fish propelled by an ionic polymer–metal composite caudal fin. *IEEE/ASME Transact Mechatron* 2010; 15: 448–459. DOI: 10.1109/tmech.2009.2027812.
 79. Yang T and Chen Z. Development of 2D maneuverable robotic fish propelled by multiple ionic polymer-metal composite artificial fins. *IEEE International Conference on Robotics and Biomimetics (ROBIO)*, 2015, pp. 255–260. DOI: 10.1109/ROBIO.2015.7418776.
 80. Zheng C, Um TI, and Bart-smith H. Bio-inspired robotic manta ray powered by ionic polymer-metal composite artificial muscles. *Int J Smart Nano Mat (UK)* 2012; 3: 296–308. DOI: 10.1080/19475411.2012.686458.
 81. Hubbard JJ, Fleming M, Palmre V, et al. Monolithic IPMC fins for propulsion and maneuvering in bioinspired underwater robotics. *IEEE J Oceanic Eng* 2014; 39: 540–551. Article. DOI: 10.1109/joe.2013.2259318.
 82. Yi XF, Chakarvarthy A, and Chen Z. Cooperative collision avoidance control of servo/IPMC driven robotic fish with back-relaxation effect. *IEEE Robot Autom Lett* 2021; 6: 1816–1823. Article. DOI: 10.1109/lra.2021.3060717.
 83. Chen Z and Tan XB. A control-oriented and physics-based model for ionic polymer-metal composite actuators. *IEEE-ASME Transact Mechatron* 2008; 13: 519–529. Article. DOI: 10.1109/tmech.2008.920021.
 84. Shintake J, Cacucciolo V, Shea H, et al. Soft biomimetic fish robot made of dielectric elastomer actuators. *Soft Robot* 2018; 5: 466–474. Article. DOI: 10.1089/soro.2017.0062.
 85. Wu Y, Alici G, Spinks GM, et al. Fast trilayer polypyrrole bending actuators for high speed applications. *Synthetic Metals* 2006; 156: 1017–1022. DOI: 10.1016/j.synthmet.2006.06.022.
 86. McGovern ST, Abbot M, Emery R, et al. Evaluation of thrust force generated for a robotic fish propelled with polypyrrole actuators. *Polym Int* 2010; 59: 357–364. DOI: 10.1002/pi.2777.
 87. McGovern S, Alici G, Truong V-T, et al. Finding NEMO (novel Electromaterial muscle oscillator): a polypyrrole powered robotic fish with real-time wireless speed and directional control. *Smart Mater Struct* 2009; 18. DOI: 10.1088/0964-1726/18/9/095009.
 88. Brochu P and Pei QB. Advances in dielectric elastomers for actuators and artificial muscles. *Macromol Rapid Commun* 2010; 31: 10–36. DOI: 10.1002/marc.200900425.
 89. Borgen MG, Washington GN, and Kinzel GL. Design and evolution of a piezoelectrically actuated miniature swimming vehicle. *IEEE/ASME Transact Mechatron* 2003; 8: 66–76. DOI: 10.1109/tmech.2003.809131.
 90. Mossi KM, Selby GV, and Bryant RG. Thin-layer composite unimorph ferroelectric driver and sensor properties. *Mater Lett* 1998; 35: 39–49. DOI: 10.1016/s0167-577x(97)00214-0.
 91. Heo S, Wiguna T, Park HC, et al. Effect of an artificial caudal fin on the performance of a biomimetic fish robot propelled by piezoelectric actuators. *J Bionic Eng* 2007; 4: 151–158. DOI: 10.1016/s1672-6529(07)60027-4.
 92. Nguyen QS, Heo S, Park HC, et al. Performance evaluation of an improved fish robot actuated by piezoceramic actuators. *Smart Mater Struct* 2010; 19. DOI: 10.1088/0964-1726/19/3/035030.
 93. Zhao QL, Liu SQ, Chen JH, et al. Fast-moving piezoelectric micro-robotic fish with double caudal fins. *Robot Auton Syst* 2021; 140: 9. Article. DOI: 10.1016/j.robot.2021.103733.

94. Hu D, Lou J, Chen T, et al. Micro thrust measurement experiment and pressure field evolution of bionic robotic fish with harmonic actuation of macro fiber composites. *Mechan Syst Signal Process* 2021; 153. DOI: 10.1016/j.ymssp.2020.107538.
95. Tan D, Wang Y-C, Kohtanen E, et al. Trout-like multifunctional piezoelectric robotic fish and energy harvester. *Bioinspirat Biomimet* 2021; 16: 046024. DOI: 10.1088/1748-3190/ac011e.
96. Govindarajan G and Sharma R. Experimental investigation on a flapping beam with smart material actuation for underwater application. *Mechan Adv Mater Struct* 2021; 28: 1020–1034. DOI: 10.1080/15376494.2019.1629047.
97. Cen L and Erturk A. Bio-inspired aquatic robotics by untethered piezohydroelastic actuation. *Bioinspirat Biomimet* 2013; 8: 13. Article. DOI: 10.1088/1748-3182/8/1/016006.
98. Marchese AD, Onal CD, and Rus D. Autonomous soft robotic fish capable of escape maneuvers using fluidic elastomer actuators. *Soft Robot* 2014; 1: 75–87. 2014/03/01. DOI: 10.1089/soro.2013.0009.
99. Chen G, Yang X, Zhang X, et al. Water hydraulic soft actuators for underwater autonomous robotic systems. *Appl Ocean Res* 2021; 109. DOI: 10.1016/j.apor.2021.102551.
100. Takada Y, Koyama K, and Usami T. Position estimation of small robotic fish based on camera information and Gyro sensors. *Robotics* 2014; 3: 149–162. DOI: 10.3390/robotics3020149.
101. Yu J, Sun F, Xu D, et al. Embedded vision-guided 3-D tracking control for robotic fish. *IEEE Transact Industr Electr* 2016; 63: 355–363. DOI: 10.1109/tie.2015.2466555.
102. Ichikizaki T and Yamamoto IIEEE. Development of robotic fish with various swimming functions. In: *5th international symposium on underwater technology/5th workshop on scientific use of submarine cables and related technologies, Tokyo, Japan, 17–20 April 2007, Vols 1 and 2*, pp. 378–383.
103. Phamduy P, LeGrand R, and Porfiri M. Robotic fish: design and characterization of an interactive iDevice-controlled robotic fish for informal science education. *IEEE Robot Automat Magaz* 2015; 22: 86–96. DOI: 10.1109/mra.2014.2381367.
104. Chuanmeng N, Lige Z, Shusheng B, et al. Development and depth control of a robotic fish mimicking cownose ray. 2012, p.814–818.
105. Yu J, Ding R, Yang Q, et al. Amphibious pattern design of a robotic fish with wheel-propeller-fin mechanisms. *J Field Robot* 2013; 30: 702–716. DOI: 10.1002/rob.21470.
106. Yan Q, Han Z, Zhang S-W, et al. Parametric research of experiments on a carangiform robotic fish. *J Bionic Eng* 2008; 5: 95–101. DOI: 10.1016/s1672-6529(08)60012-8.
107. Yu J, Chen S, Wu Z, et al. On a miniature free-swimming robotic fish with multiple sensors. *Int J Adv Robot Syst* 2017; 13: 62. DOI: 10.5772/62887.
108. Wang W, Gu D, and Xie G. Autonomous optimization of swimming gait in a fish robot with multiple onboard sensors. *IEEE Transact Syst Man Cybernet Syst* 2019; 49: 891–903. DOI: 10.1109/tsmc.2017.2683524.
109. Yen W-K, Sierra DM, and Guo J. Controlling a robotic fish to swim along a wall using hydrodynamic pressure feedback. *IEEE J Oceanic Eng* 2018; 43: 369–380. DOI: 10.1109/joe.2017.2785698.
110. Zhang L, Zhao W, Hu Y, et al. Development and depth control of biomimetic robotic fish. 2007, p.3566–3571.
111. Ye X, Su Y, Guo S, et al. Design and realization of a remote control centimeter-scale robotic fish. *2008 IEEE/ASME international conference on advanced intelligent mechatronics, Vols 1-3*. 2008, pp.25–30.
112. Tan XB, Kim D, Usher N, et al. An autonomous robotic fish for mobile sensing. In: *IEEE/RSJ international conference on intelligent robots and systems, Beijing, Peoples R China, 09–13 October 2006, vols 1–12*, pp. 5424–5429.
113. Barbera G, Lijuan P, and Xinyan D. Attitude control for a pectoral fin actuated bio-inspired robotic fish. In: *IEEE international conference on robotics and automation*, 2011, pp.526–531.
114. Wen L, Wang T, Wu G, et al. Quantitative thrust efficiency of a self-propulsive robotic fish: experimental method and hydrodynamic investigation. *IEEE/ASME Transact Mechatron* 2013; 18: 1027–1038. DOI: 10.1109/tmech.2012.2194719.
115. Wright B, Vogt DM, Wood RJ, et al. *Soft Sensors for Curvature Estimation under Water in a Soft Robotic Fish*. Piscataway, NJ: IEEE, 2019, pp. 367–371.
116. Lin Y-H, Siddall R, Schwab F, et al. Modeling and control of a soft robotic fish with integrated soft sensing. *Adv Intellig Syst* 2021. DOI: 10.1002/aisy.202000244.
117. Jusufi A, Vogt DM, Wood RJ, et al. Undulatory swimming performance and body stiffness modulation in a soft robotic fish-inspired physical model. *Soft Robot* 2017; 4: 202–210. 2017/11/29. DOI: 10.1089/soro.2016.0053.
118. Liu B, Hao L, Deng J, et al. A remote operated robotic fish with temperature sensor based on IPMC Actuator. In: *21st Chinese control and decision conference, Guilin, Peoples R China, 17–19 June 2009 2009, vols 1–6*, pp. 5730–5734.
119. Dijkgraaf S. The functioning and significance of the lateral-line organs. *Biol Rev Camb Philos Soc* 1963; 38: 51–105. 1963/02/01. DOI: 10.1111/j.1469-185x.1963.tb00654.x.
120. Mogdans J and Bleckmann H. Coping with flow: behavior, neurophysiology and modeling of the fish lateral line system. *Biol Cybern* 2012; 106: 627–642. 2012/10/27. DOI: 10.1007/s00422-012-0525-3.
121. Wang W, Zhang XX, Zhao JW, et al. Sensing the neighboring robot by the artificial lateral line of a bio-inspired robotic fish. In: *IEEE/RSJ international conference on intelligent robots and systems (IROS), Hamburg, Germany, 28 September– 02 October 2015*, pp. 1565–1570. New York: IEEE.
122. Zheng XW, Xiong ML, Xie GM, et al. Data-driven modeling for superficial hydrodynamic pressure variations of two swimming robotic fish with leader-follower formation. In: *IEEE international conference on systems, man and cybernetics (SMC) Bari, Italy, 06–09 October 2019*, pp. 4331–4336. New York: IEEE.

123. Liu G, Wang A, Wang X, et al. A review of artificial lateral line in sensor fabrication and bionic applications for robot fish. *Appl Bionics Biomech* 2016; 2016: 4732703. DOI: 10.1155/2016/4732703.
124. Wei X, Shen H, and Chen W. Review on the research of bio-hydrodynamics. *J Ship Mech* 2020; 24: 962–970.
125. Yu J, Yuan J, Wu Z, et al. Data-driven dynamic modeling for a swimming robotic fish. *IEEE Transact Industr Electr* 2016; 63: 5632–5640. DOI: 10.1109/tie.2016.2564338.
126. Liu JD and Hu HS. Biological inspiration: from carangiform fish to multi-joint robotic fish. *J Bionic Eng* 2010; 7: 35–48. DOI: 10.1016/s1672-6529(09)60184-0.
127. Liu J and Hu H. Mimicry of sharp turning behaviors in a robotic fish. Proceedings of the 2005 IEEE International Conference on Robotics and Automation, 2005, pp. 3318–3323. DOI: 10.1109/ROBOT.2005.1570622.
128. Ijspeert AJ. Central pattern generators for locomotion control in animals and robots: a review. *Neural Netw* 2008; 21: 642–653. DOI: 10.1016/j.neunet.2008.03.014.
129. Cheng JG, Stein RB, Jovanovic K, et al. Identification, localization, and modulation of neural networks for walking in the mudpuppy (*Necturus maculatus*) spinal cord. *J Neurosci* 1998; 18: 4295–4304.
130. Shun-ichi A. Characteristics of random nets of analog neuron-like elements. *IEEE Trans Syst Man Cybern (USA)* 1972; SMC-2: 643–657. DOI: 10.1109/tsmc.1972.4309193.
131. Ijspeert AJ, Crespi A, Ryzcko D, et al. From swimming to walking with a salamander robot driven by a spinal cord model. *Science* 2007; 315: 1416–1420. Article. DOI: 10.1126/science.1138353.
132. Yu J, Wu Z, Wang M, et al. CPG network optimization for a biomimetic robotic fish via PSO. *IEEE Transact Neural Networks Learn Syst* 2016; 27: 1962–1968. DOI: 10.1109/tnnls.2015.2459913.
133. Zhou C and Low KH. On-line optimization of biomimetic undulatory swimming by an experiment-based approach. *J Bionic Eng* 2014; 11: 213–225. DOI: 10.1016/s1672-6529(14)60042 -1.
134. Hu YH, Liang JH, and Wang TM. Parameter synthesis of coupled nonlinear oscillators for CPG-based robotic locomotion. *IEEE Transact Industr Electron* 2014; 61: 6183–6191. DOI: 10.1109/tie.2014.2308150.
135. Ren Q, Xu J, Fan L, et al. A GIM-based biomimetic learning approach for motion generation of a multi-joint robotic fish. *J Bionic Eng* 2013; 10: 423–433. DOI: 10.1016/s1672-6529(13)60237 -1.
136. Bal C, Koca GO, Korkmaz D, et al. CPG-based autonomous swimming control for multi-tasks of a biomimetic robotic fish. *Ocean Eng* 2019; 189. DOI: 10.1016/j.oceaneng.2019.106334.
137. Yan Z, Yang H, Zhang W, et al. Research on motion mode switching method based on CPG network reconstruction. *IEEE Access* 2020; 8: 224871–224883. DOI: 10.1109/access.2020.3045227.
138. Videler JJ. Body surface adaptations to boundary-layer dynamics. *Symposia Soci Exp Biol* 1995; 49: 1–20.
139. Dou Z, Wang J, and Chen D. Bionic research on fish scales for drag reduction. *J Bionic Eng* 2012; 9: 457–464. DOI: 10.1016/s1672-6529(11)60140-6.
140. Zhang X, Wang W, Chen S, et al. Study on perception of neighbor bionic fish based on artificial lateral line system. *Measurment Control Technol* 2016; 35: 33–37.
141. Zheng XW, Wang C, Fan RF, et al. Artificial lateral line based local sensing between two adjacent robotic fish. *Bioinspirat Biomimet* 2018; 13. DOI: 10.1088/1748-3190/aa8f2e.
142. Pollard B and Tallapragada P. Learning hydrodynamic signatures through proprioceptive sensing by bioinspired swimmers. *Bioinspirat Biomimet* 2021; 16. DOI: 10.1088/1748-3190/abd044.
143. Li L, Liu D, Deng J, et al. Fish can save energy via proprioceptive sensing. *Bioinspirat Biomimet* 2021; 16. DOI: 10.1088/1748-3190/ac165e.
144. Carryon GN and Tangorra JL. The effect of sensory feedback topology on the entrainment of a neural oscillator with a compliant foil for swimming systems. *Bioinspirat Biomimet* 2020; 15. DOI: 10.1088/1748-3190/ab76a0.
145. Li XF, Ren QY, and Xu JX. Precise speed tracking control of a robotic fish via iterative learning control. *IEEE Transact Industr Electron* 2016; 63: 2221–2228. DOI: 10.1109/tie.2015.2499719.